Signal Processing 166 (2020) 107254

Contents lists available at ScienceDirect

Signal Processing

journal homepage: www.elsevier.com/locate/sigpro

Semi-blind receivers for MIMO multi-relaying systems via rank-one tensor approximations

Bruno Sokal[a,*], André L.F. de Almeida[a], Martin Haardt[b]

[a] Department of Teleinformatics Engineering, Federal University of Ceará, Fortaleza, Brazil
[b] Communications Research Laboratory, Ilmenau University of Technology, Ilmenau, Germany

ARTICLE INFO

Article history:
Received 26 March 2019
Revised 2 July 2019
Accepted 7 August 2019
Available online 13 August 2019

Keywords:
MIMO systems
Cooperative communications
Tensor decomposition
Space-time coding
Semi-blind receiver

ABSTRACT

This paper proposes two tensor-based receivers for multiple-input multiple-output (MIMO) multi-relaying systems capable of jointly estimating the channels and symbols in a semi-blind fashion. Assuming space-time coding at the source and relay stations, we propose an orthogonal design based on a parallel factor (PARAFAC) analysis of the coding structure. Exploiting the proposed tensor codes and the multi-linear structure of the resulting received signals, we show that the data model for every relay-assisted link after space-time combining/decoding has a Kronecker structure, which can be recast as a rank-one tensor corrupted by noise. The proposed receivers combine the tensor signals for the multiple cooperative links for joint channel and symbol estimation by coupling multiple rank-one tensor approximation problems. The first one is a coupled-SVD based receiver that estimates all the involved communication channels and transmitted symbols in closed form. The second one is an iterative solution based on alternating least squares. The performances of both receivers are evaluated by means of computer simulations in a variety of system configurations. Our results show the effectiveness of the proposed receivers and its good performance-complexity trade-off in comparison with competing receivers.

1. Introduction

In modern wireless communications, cooperative diversity is a key concept to overcome the channel impairments, such as fading, shadowing, and path loss, resulting in enhanced coverage and increased system capacity [1–4]. In cooperative diversity infrastructures, multiple wireless links are established by using relay stations to help the communication between source and destination nodes [5]. As a result, a virtual multiple input multiple output (MIMO) system with increased spatial degrees of freedom is created [6].

However, for achieving the potential gains of cooperative communications, an accurate knowledge of channel state information (CSI) associated with the multiple hops involved in the communication is necessary. Moreover, the use of precoding/beamforming techniques at the source and/or relays generally requires instantaneous channel knowledge of the different links to optimize transmission [7]. In practice, the CSI is unknown and is usually estimated with the aid of training sequences. Also, in cooperative communications, especially with multiple hops, impairments such as carrier frequency offset and timing offset become present in the system. The references [8,9] present discussions and good solutions to overcome these impairments. However, dealing with carrier frequency offset and timing offset is beyond the scope of this work. We focus on the tensor-based receiver design for the multi-relaying system to compare our receivers with the state of art solutions in the literature.

In the past decade, the use of multilinear algebra for modeling MIMO wireless communications has been growing [10–17], and has resulted, more recently, in proposals of tensor-based receivers for cooperative communication systems [18–24]. The main interest has been on the use of tensor decompositions to model the received signal as well as to derive receiver algorithms exploiting multiple forms of signal diversity. Another feature of tensor-based receivers is their build in semi-blind signal and channel recovery capability, which avoids the use of bandwidth consuming training sequences for channel estimation. Most of these works rely on generalizations of parallel factors (PARAFAC) [25] and Tucker [26] decompositions or hybrids of these decompositions, such as the PARATUCK-2 [21,24], Nested-PARAFAC [22,27] and Nested-Tucker [23] decompositions. It is worth to mention the references [15,17] where the advantages of using coupled-tensor solutions for parameter estimation are presented, especially the work [17], where this coupling approach is directly applied to array signal processing.

* Corresponding author.
E-mail addresses: brunosokal@gtel.ufc.br (B. Sokal), andre@gtel.ufc.br (A.L.F. de Almeida), martin.haardt@tu-ilmenau.de (M. Haardt).

https://doi.org/10.1016/j.sigpro.2019.107254
0165-1684/

Closely related to the present work are those proposed in [18,22–24,27]. The authors of [18] develop a tensor-based channel estimation algorithm for two-way MIMO relaying systems using training sequences. In [20], channel estimation for a two-hop MIMO relaying system is addressed via PARAFAC analysis, while in [24], a supervised joint channel estimation algorithm is proposed for one-way three-hop communication systems with two relay layers. Note that both Roemer and Haardt [18] and Cavalcante et al. [24] propose pilot-assisted schemes. To avoid training sequences, in [22] the authors deal with a semi-blind joint channel and symbol estimation for a two-hop MIMO relaying system using a Nested PARAFAC modeling approach. In a more recent work [23], a generalization of Ximenes et al. [22] is proposed by adopting full space-time coding at the source and the relay in a two-hop MIMO relaying system. Therein, the authors also derive two semi-blind receivers. The first is based on alternating least squares (ALS) estimation while the second is a closed-form solution one based on a two-step least squares Kronecker product (LSKP) factorization. Both solutions in [23] have shortcomings that may limit their applicability. On the one hand, the ALS-based receiver requires the computation of matrix inverses at every iteration, while the LSKP accomplishes channel and symbol estimation in two sequential steps (2LSKP) being susceptible to error propagation. On the other hand, supervised receivers such as that of Cavalcante et al. [24] assume that the source transmits long training sequences, which we want to avoid. The idea of joint channel and symbol estimation based on a rank-one tensor modeling approach was originally proposed in [28], and have shown to be a computationally attractive solution compared to the approach of Favier et al. [23].

In this paper, we propose two semi-blind receivers, that are extensions to the approach of Sokal et al. [28] by considering multiple cooperative links in a three-hop MIMO relaying systems. We start from the same system model as in [23,28], where tensor space-time coding is used at the source and the relay stations, which results in Nested Tucker models for the signals received at the destination. We show how to convert the received signal model of each relay-assisted link into a rank-one tensor, after a pre-processing stage (space-time filtering) that exploits the multilinear structure of the space-time coding tensors. More specifically, we first propose an orthogonal design based on a PARAFAC decomposition of the space-time coding tensors with fixed rank, which are properly chosen to satisfy an orthogonality constraint. Then, by exploiting the proposed tensor codes and the multi-linear structure of the resulting received signal, we propose semi-blind receivers based on rank-one tensor approximations which yield accurate and less computationally demanding estimates of the channels and symbols, compared to competing state-of-the-art tensor-based receivers. The proposed receivers also combine the signals from different cooperative links for joint channel and symbol estimation by coupling multiple rank-one tensor approximation problems as a single problem.

In summary, the main contributions of this paper can be listed as follows:

1. We show that the joint-semi-blind channel and symbol estimation in a two-hop MIMO relaying system can be made simpler by exploiting the tensor space-time coding structure at the receiver, which allows replacing a Nested Tucker model fitting by a Kronecker approximation problem after space-time combining/decoding. More specifically, following the idea proposed in [29], we propose a rearrangement of a N-factor Kronecker approximation problem into a Nth order rank-one tensor approximation problem, the solution of which delivers estimates of the involved communication channels and transmitted symbols at high accuracy and low complexity;
2. Two semi-blind receivers are proposed that couple the tensor received signals of the multiple relay links via rank-one tensor approximation problems while exploiting cooperative diversity in different ways. The first algorithm, referred to as coupled-SVD (C-SVD), estimates all the involved communication channels and transmitted symbols in a closed form. The second solution consists of a coupled alternating least squares (C-ALS) algorithm that combines estimates from multiple cooperative links while avoiding matrix inversions due to the rank-one property of the involved signals. As will be discussed later, the C-SVD receiver becomes more attractive than the C-ALS in a low energy per symbol to noise power spectral density (E_S/N_0) regime, due to the number of iterations required for the C-ALS to converge, also in scenarios where the code length of the space-time coding tensors at the relays is small.

The rest of this paper is structured as follows. In Section 2, we present the least squares Kronecker approximation problem and link it to a rank-one tensor approximation problem. In Section 3, we describe the system model. The pre-processing stage performed by the receivers is detailed in Section 4. The proposed C-SVD and C-ALS receivers are formulated in Sections 5.1 and 5.2, respectively. Simulation results are presented in Section 6 and the paper is concluded in Section 7.

1.1. Notation and properties

Scalars are denoted by lower-case letters ($a, b, \ldots$), vectors by bold lower-case letters ($\mathbf{a}, \mathbf{b}, .$), matrices by bold upper-case letters ($\mathbf{A}, \mathbf{B}, .$), tensors are defined by calligraphic upper-case letters ($\mathcal{A}, \mathcal{B}, \ldots$). $\mathbf{A}^{\mathrm{T}}$, $\mathbf{A}\dagger$, $\mathbf{A}^{*}$, $\mathbf{A}^{\mathrm{H}}$ stand for transpose, Moore–Penrose pseudo-inverse, conjugate and Hermitian of $\mathbf{A}$, respectively. The operators $\otimes$, $\diamond$ and $\circ$ define the Kronecker, Khatri–Rao and the outer product, respectively.

For a matrix $\mathbf{A} \in \mathbb{C}^{I \times R}$, the vec$(\cdot)$ operator vectorizes a matrix by stacking its columns, i.e., vec$(\mathbf{A}) = \mathbf{a} \in \mathbb{C}^{IR \times 1}$, while unvec$(\cdot)$ does the inverse operation, i.e., unvec$(\mathbf{a}) = \mathbf{A} \in \mathbb{C}^{I \times R}$. The frontal slices of a third-order tensor $\mathcal{X} \in \mathbb{C}^{I_1 \times I_2 \times I_3}$ are matrices denoted by $\mathbf{X}_{::i_3} \in \mathbb{C}^{I_1 \times I_2}$, with $i_3 = \{1, \cdots, I_3\}$.

For an Nth order tensor $\mathcal{X} \in \mathbb{C}^{I_1 \times \cdots \times I_N}$ there are several ways to matricize it. The n-mode unfolding of $\mathcal{X}$ is the matrix defined as $\mathbf{X}_{(n)} \in \mathbb{C}^{I_n \times I_1, \ldots, I_{n-1} I_{n+1}, \ldots I_N}$. The generalized unfolding is the matrix where the rows and columns are defined by grouping a subset of dimensions. For instance, consider the case of a fourth-order tensor $\mathcal{G} \in \mathbb{C}^{I \times J \times K \times L}$, the generalized unfolding $[\mathbf{G}]_{[(1,3),(2,4)]} \in \mathbb{C}^{IK \times JL}$ is formed by grouping the first and third dimensions (I and K) along the rows while grouping the second and fourth dimensions (J and L) along the columns, see [30].

The n-mode product between a tensor $\mathcal{X} \in \mathbb{C}^{I_1 \times \cdots \times I_N}$ and a matrix $\mathbf{A} \in \mathbb{C}^{J_1 \times I_1}$ is defined as $\mathcal{Y} = \mathcal{X} \times_1 \mathbf{A}$, where $\mathcal{Y} \in \mathbb{C}^{J_1 \times I_2 \times \cdots \times I_N}$, so that $\mathbf{Y}_{(1)} = \mathbf{A}\mathbf{X}_{(1)} \in \mathbb{C}^{J_1 \times I_2 \cdots I_N}$. Consider two third-order tensors $\mathcal{X} \in \mathbb{C}^{I_1 \times R \times I_2}$ and $\mathcal{Y} \in \mathbb{C}^{R \times J_1 \times J_2}$, where the dimension of the 2-mode of $\mathcal{X}$ is equal to the dimension of the 1-mode of $\mathcal{Y}$. The (2,1)-mode contraction between these two tensors is symbolized by $\mathcal{G} = \mathcal{X} \bullet_2^1 \mathcal{Y}$, i.e., $g_{i_1 i_2 j_1 j_2} = \sum_{r=1}^{R} x_{i_1 r i_2} y_{r j_1 j_2}$, where $\mathcal{G} \in \mathbb{C}^{I_1 \times I_2 \times J_1 \times J_2}$. A rank-one third-order tensor is defined as the outer product of three vectors and is symbolized by $\mathcal{X} \in \mathbb{C}^{I_1 \times I_2 \times I_3} = \mathbf{a} \circ \mathbf{b} \circ \mathbf{c}$, with $\mathbf{a} \in \mathbb{C}^{I_1 \times 1}$, $\mathbf{b} \in \mathbb{C}^{I_2 \times 1}$, $\mathbf{c} \in \mathbb{C}^{I_3 \times 1}$. Note that vec$(\mathbf{a} \circ \mathbf{b} \circ \mathbf{c}) = \mathbf{c} \otimes \mathbf{b} \otimes \mathbf{a}$. We make use of the following properties

$$(\mathbf{A} \otimes \mathbf{B})(\mathbf{C} \otimes \mathbf{D}) = \mathbf{AC} \otimes \mathbf{BD} \tag{1}$$

$$\mathrm{vec}(\mathbf{ABC}) = (\mathbf{C}^{\mathrm{T}} \otimes \mathbf{A})\mathrm{vec}(\mathbf{B}) \tag{2}$$

$$\mathrm{vec}(\mathbf{A}\mathrm{D}_n(\mathbf{B})\mathbf{C}) = (\mathbf{C}^{\mathrm{T}} \diamond \mathbf{A})\mathbf{b}_n^{\mathrm{T}}, \tag{3}$$

where $\mathrm{D}_n(\mathbf{B})$ is a diagonal matrix formed by the nth row of $\mathbf{B}$, and $\mathbf{b}_n^{\mathrm{T}}$ is the transposition of the nth row vector of $\mathbf{B}$. Given a third-order PARAFAC tensor $\mathcal{X} = \mathcal{I}_R \times_1 \mathbf{A} \times_2 \mathbf{B} \times_3 \mathbf{C} \in \mathbb{C}^{I_1 \times I_2 \times I_3}$, its frontal slices are given by

$$\mathbf{X}_{..i_3} = \mathbf{A}\mathrm{D}_{i_3}(\mathbf{C})\mathbf{B}^{\mathrm{T}} \in \mathbb{C}^{I_1 \times I_2}, \tag{4}$$

where $i_3 = \{1, \ldots, I_3\}$, and $\mathbf{A} \in \mathbb{C}^{I_1 \times R}$, $\mathbf{B} \in \mathbb{C}^{I_2 \times R}$, $\mathbf{C} \in \mathbb{C}^{I_3 \times R}$ are the factor matrices, and R is the tensor rank of $\mathcal{X}$.

2. Kronecker product approximation

In this section, we show how to recast a three-factor Kronecker factorization problem into a third-order rank-one tensor approximation. Such a link will play a key role in the design of the proposed receivers.

Consider the following minimization problem

$$\min_{\mathbf{A},\mathbf{B}} \phi(\mathbf{A}, \mathbf{B}) = \|\mathbf{X} - \mathbf{A} \otimes \mathbf{B}\|_F, \tag{5}$$

where $\mathbf{A} \in \mathbb{C}^{I_2 \times R_2}$, $\mathbf{B} \in \mathbb{C}^{I_1 \times R_1}$ and $\mathbf{X} = \mathbf{A} \otimes \mathbf{B} + \mathbf{V} \in \mathbb{C}^{I_1 I_2 \times R_1 R_2}$, and $\mathbf{V}$ contain zero-mean uncorrelated noise. For the problem in Eq. (5), the authors in [29] proposed a solution based on a rank-one matrix approximation (via SVD) of $\overline{\mathbf{X}}$ (a permuted version of $\mathbf{X}$ constructed according to Van Loan and Pitsianis [29]). The problem in (5) becomes

$$\min_{\mathbf{a},\mathbf{b}} \phi(\mathbf{a}, \mathbf{b}) = \left\|\overline{\mathbf{X}} - \mathbf{b} \circ \mathbf{a}\right\|_F, \tag{6}$$

meaning to find the nearest rank-one matrix to $\overline{\mathbf{X}}$, where $\mathbf{a} = \mathrm{vec}(\mathbf{A}) \in \mathbb{C}^{I_2 R_2 \times 1}$ and $\mathbf{b} = \mathrm{vec}(\mathbf{B}) \in \mathbb{C}^{I_1 R_1 \times 1}$. The Kronecker approximation problem in (5) has been exploited previously in the literature. In [31], Kronecker product approximations are derived for three-dimensional (3-D) image processing applications. By linking the problems to tensor decompositions, the authors show that a Kronecker-structured matrix approximation problem can be reduced to a computationally tractable problem involving third-order tensor. This link is exploited to derive Kronecker approximation preconditioners for iterative regularization. In [32], the authors proposed a solution generalizing [29] to a Kronecker product involving N factor matrices. However, our proposed solution is directly related to rank-one tensors.

In this work, we are interested in solving this problem for $N = 3$, which is the case of the proposed MIMO multi-relaying system discussed in the following sections. To this end, consider the following problem

$$\min_{\mathbf{A},\mathbf{B},\mathbf{C}} \phi(\mathbf{A}, \mathbf{B}, \mathbf{C}) = \|\mathbf{X} - \mathbf{A} \otimes \mathbf{B} \otimes \mathbf{C}\|_F, \tag{7}$$

where $\mathbf{A} \in \mathbb{C}^{I_3 \times R_3}$, $\mathbf{B} \in \mathbb{C}^{I_2 \times R_2}$ and $\mathbf{C} \in \mathbb{C}^{I_1 \times R_1}$. The problem in (7) now becomes

$$\min_{\mathbf{a},\mathbf{b},\mathbf{c}} \phi(\mathbf{a}, \mathbf{b}, \mathbf{c}) = \|\overline{\mathbf{x}} - \mathbf{a} \otimes \mathbf{b} \otimes \mathbf{c}\|_F, \Longleftrightarrow$$
$$\min_{\mathbf{c},\mathbf{b},\mathbf{a}} \phi(\mathbf{c}, \mathbf{b}, \mathbf{a}) = \left\|\overline{\mathcal{X}} - \mathbf{c} \circ \mathbf{b} \circ \mathbf{a}\right\|_F, \tag{8}$$

where $\mathbf{a} = \mathrm{vec}(\mathbf{A}) \in \mathbb{C}^{I_3 R_3 \times 1}$, $\mathbf{b} = \mathrm{vec}(\mathbf{B}) \in \mathbb{C}^{I_2 R_2 \times 1}$, $\mathbf{c} = \mathrm{vec}(\mathbf{C}) \in \mathbb{C}^{I_1 R_1 \times 1}$. We have that $\overline{\mathbf{x}} = \mathrm{vec}(\overline{\mathbf{X}})$ and $\overline{\mathcal{X}} = \mathcal{T}\{\overline{\mathbf{x}}\} \in \mathbb{C}^{I_1 R_1 \times I_2 R_2 \times I_3 R_3}$, where the operator $\mathcal{T}\{\cdot\}$ maps the elements of $\overline{\mathbf{x}}$ into $\overline{\mathcal{X}}$, as follows

$$\overline{\mathbf{x}}_{q_1 + (q_2-1)Q_1 + (q_3-1)Q_1 Q_2} \xrightarrow[\mathcal{T}\{\cdot\}]{} \overline{\mathcal{X}}_{q_1, q_2, q_3} \tag{9}$$

where $q_i = \{1, \ldots, Q_i\}$ and $Q_i = I_i R_i$, with $i = \{1, 2, 3\}$.

Hence, finding the matrix triplet {**A, B, C**} that solves (7) is equivalent to finding the vector triplet {**a, b, c**} that solves (8), i.e., the solution of a Kronecker approximation problem can be recast as the solution to a rank-one tensor approximation problem, for which effective algorithms exist in the literature (see, e.g., [33–35]). Here we generalize the block-matrix arrangement from Van Loan and Pitsianis [29] to map $\mathbf{X}$ to $\overline{\mathcal{X}}$ resulting in a rank-one tensor approximation problem.

Let us define $\mathbf{D} = \mathbf{A} \otimes \mathbf{B} \otimes \mathbf{C} \in \mathbb{C}^{I_1 I_2 I_3 \times R_1 R_2 R_3}$. Due to its Kronecker structure, this matrix can be viewed in three different ways (block-division): First, as a block matrix of size $I_2 I_3 \times R_2 R_3$, each element of which being a matrix of size $I_1 \times R_1$. Second, as block matrix of size $I_3 \times R_3$, each element being a matrix of size $I_1 I_2 \times R_1 R_2$ formed by the block $\mathbf{B} \otimes \mathbf{C}$. Third, the same matrix can be viewed as the total matrix $\mathbf{D}$. Our goal is to rearrange the elements of $\mathbf{D}$ into a matrix $\overline{\mathbf{D}}$ whose vectorization can be factored by a Kronecker product of three vectors, i.e., $\overline{\mathbf{d}} = \mathbf{a} \otimes \mathbf{b} \otimes \mathbf{c}$, where $\overline{\mathbf{d}} = \mathrm{vec}(\overline{\mathbf{D}}) \in \mathbb{C}^{I_1 R_1 I_2 R_2 I_3 R_3 \times 1}$. Fig. 1 provides an illustration of this mapping, where each block $\mathbf{P}^{(1)}_{(i,j)}$ is a matrix of size $I_1 \times R_1$, each block $\mathbf{P}^{(2)}_{(k,l)}$ is a matrix of size $I_1 I_2 \times R_1 R_2$, and the block $\mathbf{P}^{(3)}$ is the total matrix of size $I_1 I_2 I_3 \times R_1 R_2 R_3$. The upper index n of $\mathbf{P}^{(n)}_{(i,j)}$ indicates the block division, with $n \in \{1, 2, 3\}$. The lower indices (i, j) indicate the position of the matrix block $\mathbf{P}^{(n)}_{(i,j)}$ inside the matrix block $\mathbf{P}^{(n+1)}_{(k,l)}$, where $i = \{1 \cdots I_2\}$, $j = \{1 \cdots R_2\}$, $k = \{1 \cdots I_3\}$, $l = \{1 \cdots R_3\}$, and $n + 1 \leq 3$.

Let $\overline{\mathbf{G}}_{(k,l)}$ be a matrix of size $I_1 R_1 \times I_2 R_2$, each column of which is the vectorization of the matrix block $\mathbf{P}^{(1)}_{(i,j)}$ (defined as $\mathbf{p}^{(1)}_{(i,j)}$ with size $I_1 R_1 \times 1$) belonging to the bigger block $\mathbf{P}^{(2)}_{(k,l)}$. We have

$$\overline{\mathbf{G}}_{(k,l)} = [\mathbf{p}^{(1)}_{(1,1)}, \ldots, \mathbf{p}^{(1)}_{(I_2,1)}, \ldots, \mathbf{p}^{(1)}_{(I_2,R_2)}]_{\mathbf{P}^{(2)}_{(k,l)}}. \tag{10}$$

Finally, we define $\overline{\mathbf{D}}$ of size $I_1 R_1 I_2 R_2 \times I_3 R_3$ by collecting the column vectors $\overline{\mathbf{g}}_{(k,l)} = \mathrm{vec}(\overline{\mathbf{G}}_{(k,l)})$ of size $I_1 R_1 I_2 R_2 \times 1$, as follows

$$\overline{\mathbf{D}} = [\overline{\mathbf{g}}_{(1,1)}, \ldots, \overline{\mathbf{g}}_{(I_3,1)}, \ldots, \overline{\mathbf{g}}_{(I_3,R_3)}]_{\mathbf{P}^{(3)}}. \tag{11}$$

By applying the $\mathrm{vec}(\cdot)$ operator, we get $\overline{\mathbf{d}} = \mathbf{a} \otimes \mathbf{b} \otimes \mathbf{c}$. Since the Kronecker product is directly related to the outer product, it follows that

$$\overline{\mathcal{D}} = \mathbf{c} \circ \mathbf{b} \circ \mathbf{a}, \tag{12}$$

where $\overline{\mathcal{D}} = \mathcal{T}\{\overline{\mathbf{d}}\} \in \mathbb{C}^{I_1 R_1 \times I_2 R_2 \times I_3 R_3}$ is a third-order rank-one tensor formed by the "tensorizing" $\overline{\mathbf{d}} \in \mathbb{C}^{I_1 R_1 I_2 R_2 I_3 R_3 \times 1}$. Note that the rank-one tensor formulation described in this section can be extended to higher orders from a Kronecker factorization involving $N > 3$ matrices, but we keep the focus on the case $N = 3$ due to the present context.

$$\mathbf{D} = \begin{bmatrix} \begin{bmatrix} [\mathbf{P}^{(1)}_{(1,1)}] & \cdots & [\mathbf{P}^{(1)}_{(1,R_2)}] \\ \vdots & \ddots & \vdots \\ [\mathbf{P}^{(1)}_{(I_2,1)}] & \cdots & [\mathbf{P}^{(1)}_{(I_2,R_2)}] \end{bmatrix}_{\mathbf{P}^{(2)}_{(1,1)}} & \cdots & \begin{bmatrix} [\mathbf{P}^{(1)}_{(1,1)}] & \cdots & [\mathbf{P}^{(1)}_{(1,R_2)}] \\ \vdots & \ddots & \vdots \\ [\mathbf{P}^{(1)}_{(I_2,1)}] & \cdots & [\mathbf{P}^{(1)}_{(I_2,R_2)}] \end{bmatrix}_{\mathbf{P}^{(2)}_{(1,R_3)}} \\ \vdots & \ddots & \vdots \\ \begin{bmatrix} [\mathbf{P}^{(1)}_{(1,1)}] & \cdots & [\mathbf{P}^{(1)}_{(1,R_2)}] \\ \vdots & \ddots & \vdots \\ [\mathbf{P}^{(1)}_{(I_2,1)}] & \cdots & [\mathbf{P}^{(1)}_{(I_2,R_2)}] \end{bmatrix}_{\mathbf{P}^{(2)}_{(I_3,1)}} & \cdots & \begin{bmatrix} [\mathbf{P}^{(1)}_{(1,1)}] & \cdots & [\mathbf{P}^{(1)}_{(1,R_2)}] \\ \vdots & \ddots & \vdots \\ [\mathbf{P}^{(1)}_{(I_2,1)}] & \cdots & [\mathbf{P}^{(1)}_{(I_2,R_2)}] \end{bmatrix}_{\mathbf{P}^{(2)}_{(I_3,R_3)}} \end{bmatrix}_{\mathbf{P}^{(3)}}$$

Fig. 1. Matrix **D** and its block structure.

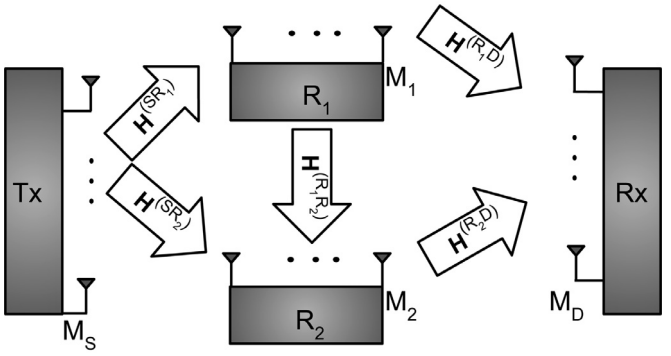

Fig. 2. MIMO multi-relaying system.

3. System model

We consider a multi-relaying MIMO system where the source is assisted by two half-duplex relays using the AF protocol. In this system, M_S denotes the number of transmit antennas at the source and M_D is the number of receive antennas at the destination. Relay 1 is equipped with M_1 antennas, from which M_{S_1} antennas are used for transmission and M_{R_1} for reception. Likewise, M_2 denotes the total number of antennas at Relay 2, with M_{S_2} transmit antennas and M_{R_2} receive antennas. Fig. 2 provides an overview of the system model. The transmission of information from the source to the destination via the multiple relays involves a three-phase transmission scheme. In the following, the tensor-based signal model for each phase is formulated using tensor n-mode product, slice, contraction operations. This formalism is essential to obtain the received signal model at the destination as a basis for deriving the proposed semi-blind receivers. It is important to mention that all the processing is performed at the destination, i.e., the relay station only codes the signal and forwards it. Moreover, for simplicity, we assume perfect timing synchronization at the relays and destination.

Phase 1. The source transmits the signal to Relay 1 and Relay 2. The symbol matrix $\mathbf{S} \in \mathbb{C}^{N\times R}$ contains R data streams of N symbols each. These data streams are encoded at the source by means of a space-time coding tensor $\mathcal{C} \in \mathbb{C}^{M_S\times R\times P}$, where P is the code length. The transmitted signal tensor $\mathcal{X}^{(S)} \in \mathbb{C}^{M_S\times N\times P}$ is given by the following n-mode product and slice matrix product as:

$$\mathcal{X}^{(S)} = \mathcal{C} \times_2 \mathbf{S} \tag{13}$$

$$\mathbf{X}^{(S)}_{..p} = \mathbf{C}_{..p}\mathbf{S}^{\mathrm{T}} \in \mathbb{C}^{M_S\times N}. \tag{14}$$

Each symbol is repeated P times over the M_S antennas creating a space-time redundancy, i.e., we have P time-slots with N symbols each. Considering $\mathbf{H}^{(SR_1)} \in \mathbb{C}^{M_{R_1}\times M_S}$ as the channel between the source and the Relay 1, and $\mathbf{H}^{(SR_2)} \in \mathbb{C}^{M_{R_2}\times M_S}$ as the channel between the source and Relay 2, the signal received at Relay 1 is the tensor $\mathcal{X}^{(SR_1)} \in \mathbb{C}^{M_{R_1}\times N\times P}$ and can be written, in n-mode product and slice notation, respectively, as

$$\mathcal{X}^{(SR_1)} = \mathcal{X}^{(S)} \times_1 \mathbf{H}^{(SR_1)} + \mathcal{V}^{(SR_1)} \tag{15}$$

$$\mathbf{X}^{(SR_1)}_{..p} = \mathbf{H}^{(SR_1)}\mathbf{X}^{(S)}_{..p} + \mathbf{V}^{(SR_1)}_{..p} \in \mathbb{C}^{M_{R_1}\times N}, \tag{16}$$

where $\mathcal{V}^{(SR_1)} \in \mathbb{C}^{M_{R_1}\times N\times P}$ is the additive white Gaussian noise (AWGN) at Relay 1. The signal received at Relay 2, $\mathcal{X}^{(SR_2)} \in \mathbb{C}^{M_{R_2}\times N\times P}$ is given by

$$\mathcal{X}^{(SR_2)} = \mathcal{X}^{(S)} \times_1 \mathbf{H}^{(SR_2)} + \mathcal{V}^{(SR_2)} \tag{17}$$

$$\mathbf{X}^{(SR_2)}_{..p} = \mathbf{H}^{(SR_2)}\mathbf{X}^{(S)}_{..p} + \mathbf{V}^{(SR_2)}_{..p} \in \mathbb{C}^{M_{R_2}\times N}, \tag{18}$$

where $\mathcal{V}^{(SR_2)} \in \mathbb{C}^{M_{R_2}\times N\times P}$ is the AWGN tensor at Relay 2.

Phase 2. Since we are considering half-duplex nodes, the source stays silent and only one relay transmits in this phase. Without loss of generality, let us assume that Relay 1 transmits and Relay 2 stays in silent. In this case, the signal $\mathcal{X}^{(SR_1)}$ received in the previous phase by Relay 1, is coded and forwarded to Relay 2 and to the destination. A space-time coding tensor $\mathcal{W} \in \mathbb{C}^{M_{S_1}\times M_{R_1}\times J}$ is used for this purpose, assuming M_{S_1} transmit antennas. Similarly to Phase 1, a space-time spreading structure is created, having now J frames, each with P time-slots. Defining $\mathbf{H}^{(R_1R_2)} \in \mathbb{C}^{M_{R_2}\times M_{S_1}}$ as the channel connecting Relay 1 and Relay 2, and $\mathbf{H}^{(R_1D)} \in \mathbb{C}^{M_D\times M_{S_1}}$ as the channel between Relay 1 and the destination, the signal received at Relay 2, $\mathcal{X}^{(SR_1R_2)} \in \mathbb{C}^{M_{R_2}\times J\times N\times P}$ is given by

$$\begin{aligned}\mathcal{X}^{(SR_1R_2)} &= (\mathcal{W} \bullet^1_2 \mathcal{X}^{(SR_1)}) \times_1 \mathbf{H}^{(R_1R_2)} + \mathcal{V}^{(SR_1R_2)} \\ &= (\mathcal{W} \times_1 \mathbf{H}^{(R_1R_2)}) \bullet^1_2 \mathcal{X}^{(SR_1)} + \mathcal{V}^{(SR_1R_2)} \\ &= \bar{\mathcal{H}}^{(R_1R_2)} \bullet^1_2 \mathcal{X}^{(SR_1)} + \mathcal{V}^{(SR_1R_2)}\end{aligned} \tag{19}$$

$$\mathbf{X}^{(SR_1R_2)}_{.j.p} = \mathbf{H}^{(R_1R_2)}\mathbf{W}_{..j}\mathbf{X}^{(SR_1)}_{..p} + \mathbf{V}^{(SR_1R_2)}_{.j.p} \in \mathbb{C}^{M_{R_2}\times N}, \tag{20}$$

where $\mathcal{V}^{(SR_1R_2)} \in \mathbb{C}^{M_{R_2}\times J\times N\times P}$ is the AWGN at Relay 2 (in Phase 2), while $\bar{\mathcal{H}}^{(R_1R_2)} = \mathcal{W} \times_1 \mathbf{H}^{(R_1R_2)} \in \mathbb{C}^{M_{R_2}\times M_{R_1}\times J}$ is the effective channel tensor. The signal $\mathcal{X}^{(SR_1D)} \in \mathbb{C}^{M_D\times J\times N\times P}$ received at the destination can be written as

$$\mathcal{X}^{(SR_1D)} = \bar{\mathcal{H}}^{(R_1D)} \bullet^1_2 \mathcal{X}^{(SR_1)} + \mathcal{V}^{(SR_1D)} \tag{21}$$

$$\mathbf{X}^{(SR_1D)}_{.j.p} = \mathbf{H}^{(R_1D)}\mathbf{W}_{..j}\mathbf{X}^{(SR_1)}_{..p} + \mathbf{V}^{(SR_1D)}_{.j.p} \in \mathbb{C}^{M_D\times N}, \tag{22}$$

where $\mathcal{V}^{(SR_1D)} \in \mathbb{C}^{M_D\times J\times N\times P}$ is the AWGN at the destination, and $\bar{\mathcal{H}}^{(R_1D)} = \mathcal{W} \times_1 \mathbf{H}^{(R_1D)} \in \mathbb{C}^{M_D\times M_{R_1}\times J}$ is the effective channel tensor.

Phase 3. Now, the source and Relay 1 stay silent while Relay 2 transmits the signal received in Phase 1 ($\mathcal{X}^{(SR_2)}$) and in Phase 2 ($\mathcal{X}^{(SR_1R_2)}$) to the destination. For this transmission, the Relay 2 concatenates the signals $\mathcal{X}^{(SR_2)}$ along the second mode of the tensor $\mathcal{X}^{(SR_1R_2)}$ as follows

$$\begin{aligned}&\overline{\mathcal{X}} = \mathcal{X}^{(SR_1R_2)} \sqcup_2 \mathcal{X}^{(SR_2)} \in \mathbb{C}^{M_{R_2}\times(J+1)\times N\times P} \\ &\text{where } \overline{\mathcal{X}}_{.(1:J)..} = \mathcal{X}^{(SR_1R_2)} \in \mathbb{C}^{M_{R_2}\times J\times N\times P} \\ &\qquad \overline{\mathcal{X}}_{.(J+1)..} = \mathcal{X}^{(SR_2)} \in \mathbb{C}^{M_{R_2}\times 1\times N\times P}.\end{aligned} \tag{23}$$

The concatenated signal is coded by means of a space-time coding tensor $\mathcal{T} \in \mathbb{C}^{M_{S_2}\times M_{R_2}\times K}$ and forwarded to the destination using M_{S_2} transmit antennas. The coding tensor introduces an additional space-time spreading to the forwarded signals, by coding information across K super-frames. This results in $P(J+1)K$ channel uses. Let $\mathbf{H}^{(R_2D)} \in \mathbb{C}^{M_D\times M_{S_2}}$ be the channel between Relay 2 and the destination. The signals received at the destination $\overline{\mathcal{X}}^{(SR_1R_2D)} \in \mathbb{C}^{M_D\times K\times(J+1)\times N\times P}$ are then given by

$$\overline{\mathcal{X}}^{(SR_1R_2D)} = \bar{\mathcal{H}}^{(R_2D)} \bullet^1_2 \overline{\mathcal{X}} + \overline{\mathcal{V}}^{(SR_1R_2D)} \tag{24}$$

$$\overline{\mathbf{X}}^{(SR_1R_2D)}_{.k(j+1).p} = \mathbf{H}^{(R_2D)}\mathbf{T}_{..k}\overline{\mathbf{X}}_{.(j+1).p} + \overline{\mathbf{V}}^{(SR_1R_2D)}_{.k(j+1).p} \in \mathbb{C}^{M_D\times N} \tag{25}$$

where $\overline{\mathcal{V}}^{(SR_1R_2D)} \in \mathbb{C}^{M_D\times K\times(J+1)\times N\times P}$ is the AWGN at the destination, and $\bar{\mathcal{H}}^{(R_2D)} = \mathcal{T} \times_1 \mathbf{H}^{(R_2D)} \in \mathbb{C}^{M_D\times M_{R_2}\times K}$ is the effective channel.

The goal of the proposed receiver is to combine the three tensor signals at the destination, namely $\mathcal{X}^{(SR_1D)}$, $\mathcal{X}^{(SR_2D)}$, and $\mathcal{X}^{(SR_1R_2D)}$. By combining all tensor signals coherently at the destination, cooperative diversity is exploited to jointly estimate the symbols and channel matrices, as will be shown later.

4. Pre-processing stage

This section discusses the pre-processing stage applied before the channel and symbol estimation. It consists of a space-time filtering that exploits the knowledge and the multi-linear structure of the coding tensors ($\mathcal{C}$, $\mathcal{W}$ and $\mathcal{T}$).

First, let us consider the signal $\mathcal{X}^{(SR_1D)}$ received at the destination from Relay 1 during Phase 2. From Eq. (22), ignoring the noise term, and replacing $\mathbf{X}_{..p}^{(SR_1)}$ as in Eq. (16), we have

$$\mathbf{X}_{.j.p}^{(SR_1D)} = \mathbf{H}^{(R_1D)}\mathbf{W}_{..j}\mathbf{H}^{(SR_1)}\mathbf{C}_{..p}\mathbf{S}^{\mathrm{T}}. \tag{26}$$

Making use of Property (2), and defining $\mathbf{x}_{j,p}^{(SR_1D)} = \mathrm{vec}(\mathbf{X}_{.j.p}^{(SR_1D)})$, yields

$$\begin{aligned}\mathbf{x}_{.j.p}^{(SR_1D)} &= \left(\mathbf{S}\otimes\mathbf{H}^{(R_1D)}\right)\mathrm{vec}\left(\mathbf{W}_{..j}\mathbf{H}^{(SR_1)}\mathbf{C}_{..p}\right)\\ &= \left(\mathbf{S}\otimes\mathbf{H}^{(R_1D)}\right)\left(\mathbf{C}_{..p}^{\mathrm{T}}\otimes\mathbf{W}_{..j}\right)\mathrm{vec}\left(\mathbf{H}^{(SR_1)}\right)\\ &= \left(\mathrm{vec}\left(\mathbf{H}^{(SR_1)}\right)^{\mathrm{T}}\otimes\mathbf{S}\otimes\mathbf{H}^{(R_1D)}\right)\mathrm{vec}\left(\mathbf{C}_{..p}^{\mathrm{T}}\otimes\mathbf{W}_{..j}\right).\end{aligned}$$

Let us define $\mathbf{Y}^{(SR_1D)}\in\mathbb{C}^{M_DN\times M_{S_1}RM_{R_1}M_S}$ the matrix

$$\mathbf{Y}^{(SR_1D)} = \mathrm{vec}(\mathbf{H}^{(SR_1)})^{\mathrm{T}}\otimes\mathbf{S}\otimes\mathbf{H}^{(R_1D)}, \tag{27}$$

by collecting the JP vectors $\{\mathbf{x}_{.j.p}^{(SR_1D)}\}$, $j=1,\dots,J$, $p=1,\dots,P$ as column vectors, we form $[\mathbf{X}^{(SR_1D)}]_{([1,3],[2,4])}\in\mathbb{C}^{M_DN\times JP}$, which is a generalized unfolding of $\mathcal{X}^{(SR_1D)}$, that can be written as

$$\begin{aligned}&[\mathbf{X}^{(SR_1D)}]_{([1,3],[2,4])} = [\mathbf{Y}^{(SR_1D)}\mathrm{vec}(\mathbf{C}_{..1}^{\mathrm{T}}\otimes\mathbf{W}_{..1}),\dots,\\ &\mathbf{Y}^{(SR_1D)}\mathrm{vec}(\mathbf{C}_{..P}^{\mathrm{T}}\otimes\mathbf{W}_{..J})] = \mathbf{Y}^{(SR_1D)}\mathbf{Z}^{(1)},\end{aligned} \tag{28}$$

where $\mathbf{Z}^{(1)}\in\mathbb{C}^{M_{S_1}RM_{R_1}M_S\times JP}$ is the effective coding matrix whose columns are $\{\mathrm{vec}(\mathbf{C}_{..p}^{\mathrm{T}}\otimes\mathbf{W}_{..j})\}$, $j=1,\dots,J$, $p=1,\dots,P$, representing the space-time filter. Adding the noise term in Eq. (28) we have

$$[\mathbf{X}^{(SR_1D)}]_{([1,3],[2,4])} = \mathbf{Y}^{(SR_1D)}\mathbf{Z}^{(1)} + [\mathbf{V}'^{(SR_1D)}]_{([1,3],[2,4])}, \tag{29}$$

where $[\mathbf{V}'^{(SR_1D)}]_{([1,3],[2,4])}$ is a generalized unfolding of the global noise tensor $\mathcal{V}'^{(SR_1D)}\in\mathbb{C}^{M_D\times J\times N\times P}$, which is composed by the noise term $\mathcal{V}^{(SR_1)}$ filtered by $\bar{\mathcal{H}}^{(R_1D)}$ and added to the $\mathcal{V}^{(SR_1D)}$ at the destination. The tensor $\mathcal{V}'^{(SR_1D)}$ can be expressed as

$$\mathcal{V}'^{(SR_1D)} = (\bar{\mathcal{H}}^{(R_1D)}\bullet_2^1\mathcal{V}^{(SR_1)}) + \mathcal{V}^{(SR_1D)}\in\mathbb{C}^{M_D\times J\times N\times P}.$$

Now, consider the signals $\overline{\mathcal{X}}^{(SR_1R_2D)}$ at the destination coming from Relay 2, defined in Eq. (24). Note that this tensor signal concatenates contributions from Relay 2 in Phases 1 and 2 (cf. Eq. (23)). More specifically, we have $\overline{\mathcal{X}}^{(SR_1R_2D)} = \bar{\mathcal{H}}^{(R_2D)}\bullet_2^1\left(\mathcal{X}^{(SR_1R_2)}\sqcup_2\mathcal{X}^{(SR_2)}\right)\in\mathbb{C}^{M_D\times K\times(J+1)\times N\times P}$. The destination extracts these two signals from $\overline{\mathcal{X}}^{(SR_1R_2D)}$ by separating the first J tensor slices to form the tensor signal $\mathcal{X}^{(SR_1R_2D)}\in\mathbb{C}^{M_D\times K\times J\times N\times P}$, while the $(J+1)$th slice is used to form the tensor signal $\mathcal{X}^{(SR_2D)}\in\mathbb{C}^{M_D\times K\times N\times P}$.

In a way similar to Eq. (25) and using Eq. (20), we can write the noiseless signal $\mathcal{X}^{(SR_1R_2D)}$ in matrix slice notation as follows

$$\begin{aligned}\mathbf{X}_{.kj.p}^{(SR_1R_2D)} &= \mathbf{H}^{(R_2D)}\mathbf{T}_{..k}\mathbf{X}_{.j.p}^{(SR_1R_2)}\\ &= \mathbf{H}^{(R_2D)}\mathbf{T}_{..k}\mathbf{H}^{(R_1R_2)}\mathbf{W}_{..j}\mathbf{X}_{..p}^{(SR_1)}\\ &= \mathbf{H}^{(R_2D)}\mathbf{T}_{..k}\mathbf{H}^{(R_1R_2)}\mathbf{W}_{..j}\mathbf{H}^{(SR_1)}\mathbf{C}_{..p}\mathbf{S}^{\mathrm{T}}.\end{aligned} \tag{30}$$

Applying Property (2) multiple times, and defining $\mathbf{x}_{k,j,p} = \mathrm{vec}(\mathbf{X}_{.kj.p}^{(SR_1R_2D)})$ yields

$$\begin{aligned}\mathbf{x}_{k,j,p} &= \left(\mathbf{S}\otimes\mathbf{H}^{(R_2D)}\right)\mathrm{vec}\left(\mathbf{T}_{..k}\mathbf{H}^{(R_1R_2)}\mathbf{W}_{..j}\mathbf{H}^{(SR_1)}\mathbf{C}_{..p}\right)\\ &= \left(\mathbf{S}\otimes\mathbf{H}^{(R_2D)}\right)\left(\mathbf{C}_{..p}^{\mathrm{T}}\otimes\mathbf{T}_{..k}\right)\mathrm{vec}\left(\mathbf{H}^{(R_1R_2)}\mathbf{W}_{..j}\mathbf{H}^{(SR_1)}\right)\\ &= \left(\mathbf{S}\otimes\mathbf{H}^{(R_2D)}\right)\left(\mathbf{C}_{..p}^{\mathrm{T}}\otimes\mathbf{T}_{..k}\right)\left(\mathbf{H}^{(SR_1)\mathrm{T}}\otimes\mathbf{H}^{(R_1R_2)}\right)\mathrm{vec}\left(\mathbf{W}_{..j}\right).\end{aligned}$$

By collecting all the J frames, we get

$$\mathbf{X}_{.k.p} = \left(\mathbf{S}\otimes\mathbf{H}^{(R_2D)}\right)\left(\mathbf{C}_{..p}^{\mathrm{T}}\otimes\mathbf{T}_{..k}\right)\left(\mathbf{H}^{(SR_1)\mathrm{T}}\otimes\mathbf{H}^{(R_1R_2)}\right)\mathbf{W}_{(3)}^{\mathrm{T}}\in\mathbb{C}^{M_DN\times J}, \tag{31}$$

where $\mathbf{W}_{(3)}\in\mathbb{C}^{M_{S_1}M_{R_1}\times J}$ is the 3-mode unfolding of the space-time coding tensor $\mathcal{W}\in\mathbb{C}^{M_{S_1}\times M_{R_1}\times J}$, which is a matrix whose columns are $\{\mathrm{vec}(\mathbf{W}_{..j})\}$, $j=1,\dots,J$. Defining $\mathbf{X}'_{.k.p} = \mathbf{X}_{.k.p}\mathbf{W}_{(3)}^{*}\in\mathbb{C}^{M_DN\times M_{S_1}M_{R_1}}$, yields

$$\mathbf{X}'_{.k.p} = (\mathbf{S}\otimes\mathbf{H}^{(R_2D)})(\mathbf{C}_{..p}^{\mathrm{T}}\otimes\mathbf{T}_{..k})(\mathbf{H}^{(SR_1)\mathrm{T}}\otimes\mathbf{H}^{(R_1R_2)}). \tag{32}$$

Applying Property (2) in Eq. (32), with $\mathbf{x}'_{k,p} = \mathrm{vec}(\mathbf{X}'_{.k.p})$, yields

$$\mathbf{x}'_{k,p} = (\mathbf{H}^{(SR_1)}\otimes\mathbf{H}^{(R_1R_2)\mathrm{T}}\otimes\mathbf{S}\otimes\mathbf{H}^{(R_2D)})\mathrm{vec}(\mathbf{C}_{..p}^{\mathrm{T}}\otimes\mathbf{T}_{..k}).$$

Let us define $\mathbf{Y}^{(SR_1R_2D)}\in\mathbb{C}^{M_DNM_{S_1}M_{R_1}\times M_{S_2}RM_{R_2}M_S}$

$$\mathbf{Y}^{(SR_1R_2D)} = \mathbf{H}^{(SR_1)}\otimes\mathbf{H}^{(R_1R_2)\mathrm{T}}\otimes\mathbf{S}\otimes\mathbf{H}^{(R_2D)}, \tag{33}$$

by collecting the KP vectors $\{\mathbf{x}'_{k,p}\}$, $k=1,\dots,K$, $p=1,\dots,P$ as column vectors, we form the matrix $[\mathbf{X}'^{(SR_1R_2D)}]_{([1,4,3],[2,5])}\in\mathbb{C}^{M_DNM_{S_1}M_{R_1}\times KP}$,

$$\begin{aligned}&[\mathbf{X}'^{(SR_1R_2D)}]_{([1,4,3],[2,5])} = [\mathbf{Y}^{(SR_1R_2D)}\mathrm{vec}(\mathbf{C}_{..1}^{\mathrm{T}}\otimes\mathbf{T}_{..1}),\dots,\\ &\mathbf{Y}^{(SR_1R_2D)}\mathrm{vec}(\mathbf{C}_{..P}^{\mathrm{T}}\otimes\mathbf{T}_{..K})] = \mathbf{Y}^{(SR_1R_2D)}\mathbf{Z}^{(2)},\end{aligned}$$

where $\mathbf{Z}^{(2)}\in\mathbb{C}^{M_{S_2}RM_{R_2}M_S\times KP}$ is the effective coding matrix whose columns are $\{\mathrm{vec}(\mathbf{C}_{..p}^{\mathrm{T}}\otimes\mathbf{T}_{..k})\}$, $k=1,\dots,K$, $p=1,\dots,P$, representing the space-time filter.

Note that $[\mathbf{X}'^{(SR_1R_2D)}]_{([1,4,3],[2,5])}$ also can be viewed as the generalized unfolding of the following filtered tensor

$$\mathcal{X}'^{(SR_1R_2D)} = \mathcal{X}^{(SR_1R_2D)}\times_3\mathbf{W}_{(3)}^{\mathrm{H}}\in\mathbb{C}^{M_D\times K\times M_{S_1}M_{R_1}\times N\times P}.$$

Now, taking into account the noise term, we have

$$[\mathbf{X}'^{(SR_1R_2D)}]_{([1,4,3],[2,5])} = \mathbf{Y}^{(SR_1R_2D)}\mathbf{Z}^{(2)} + [\mathbf{V}'^{(SR_1R_2D)}]_{([1,4,3],[2,5])}, \tag{34}$$

where $[\mathbf{V}'^{(SR_1R_2D)}]_{([1,4,3],[2,5])}$ is the generalized unfolding of the global noise tensor filtered by $\mathbf{W}_{(3)}^{\mathrm{T}}$, given by

$$\begin{aligned}\mathcal{V}'^{(SR_1R_2D)} = &\left[\bar{\mathcal{H}}^{(R_2D)}\bullet_2^1\left[(\bar{\mathcal{H}}^{(R_1R_2)}\bullet_2^1\mathcal{V}^{(SR_1)}) + \mathcal{V}^{(SR_1R_2)}\right] + \mathcal{V}^{(SR_1R_2D)}\right]\\ &\times_3\mathbf{W}_{(3)}^{\mathrm{H}}\in\mathbb{C}^{M_D\times K\times M_{S_1}M_{R_1}\times N\times P}.\end{aligned}$$

From Eqs. (29) and (27), we can formulate the following three-factor Kronecker approximation problem

$$\min_{\mathbf{H}^{(SR_1)},\mathbf{S},\mathbf{H}^{(R_1D)}}\left\|\hat{\mathbf{Y}}^{(SR_1D)} - \mathrm{vec}(\mathbf{H}^{(SR_1)})^{\mathrm{T}}\otimes\mathbf{S}\otimes\mathbf{H}^{(R_1D)}\right\|_F, \tag{35}$$

where the solution

$$\hat{\mathbf{Y}}^{(SR_1D)} = [\mathbf{X}^{(SR_1D)}]_{([1,3],[2,4])}\mathbf{Z}^{(1)\mathrm{H}} \tag{36}$$

is the received signal tensor filtered by the effective coding matrix $\mathbf{Z}^{(1)}$. Likewise, from Eqs. (34) and (33), we can formulate the following four-factor Kronecker approximation problem,

$$\min_{\mathbf{H}^{(SR_1)},\mathbf{H}^{(R_1R_2)},\mathbf{S},\mathbf{H}^{(R_2D)}}\left\|\hat{\mathbf{Y}}^{(SR_1R_2D)} - \mathbf{H}^{(SR_1)}\otimes\mathbf{H}^{(R_1R_2)\mathrm{T}}\otimes\mathbf{S}\otimes\mathbf{H}^{(R_2D)}\right\|_F. \tag{37}$$

The solution of (37) is given by

$$\hat{\mathbf{Y}}^{(SR_1R_2D)} = [\mathbf{X}^{(SR_1R_2D)}]_{([1,4,3],[2,5])}\mathbf{Z}^{(2)\mathrm{H}}, \tag{38}$$

which corresponds to received signal tensor at the destination filtered by the effective coding matrix $\mathbf{Z}^{(2)}$.

We design $\mathbf{Z}^{(1)}\in\mathbb{C}^{M_{S_1}RM_{R_1}M_S\times JP}$ and $\mathbf{Z}^{(2)}\in\mathbb{C}^{M_{S_2}RM_{R_2}M_S\times JP}$ as semi-unitary matrices, i.e., $\mathbf{Z}^{(i)}\mathbf{Z}^{(i)\mathrm{H}} = \mathbf{I}_{M_{S_i}RM_{R_i}M_S}$, $i=1,2$. As shown in the Appendix A, if a PARAFAC decomposition is assumed for the coding tensors, then $\mathbf{Z}^{(1)}$ and $\mathbf{Z}^{(2)}$ are 3-mode unfoldings of effective space-time coding tensors representing a combined source-relay coding operation. Interestingly, these effective coding tensors

also satisfy a PARAFAC decomposition structure, which greatly simplifies the receiver design. Note that a semi-unitary property is also assumed for $\mathbf{W}_{(3)}^{\mathrm{T}}$, defined in Eq (31). For the reader's convenience, the details about the design of the space-time coding tensors and the proof of the semi-unitary properties of $\mathbf{Z}^{(1)}$, $\mathbf{Z}^{(2)}$, and $\mathbf{W}_{(3)}^{\mathrm{T}}$ are given, respectively, in Appendix A and Appendix B.

Now, we capitalize on the conceptual link between the Kronecker product approximation (7) and the rank-one tensor approximation (8). By applying the block-matrix rearrangements introduced in Section 2, we map the matrix $\hat{\mathbf{Y}}^{(SR_1D)}$ to a third-order tensor $\mathcal{P}^{(SR_1D)} \in \mathbb{C}^{M_D M_{S_1} \times NR \times M_{R_1} M_S}$ which approximately has rank-one, i.e.,

$$\mathcal{P}^{(SR_1D)} \approx \mathbf{h}^{(R_1D)} \circ \mathbf{s} \circ \mathbf{h}^{(SR_1)}. \tag{39}$$

In a similar way, for the received signal tensor $\mathcal{X}^{(SR_2D)}$, we can find an approximation to a rank-one tensor $\mathcal{P}^{(SR_2D)} \in \mathbb{C}^{M_D M_{S_2} \times NR \times M_{R_2} M_S}$ given by

$$\mathcal{P}^{(SR_2D)} \approx \mathbf{h}^{(R_2D)} \circ \mathbf{s} \circ \mathbf{h}^{(SR_2)}. \tag{40}$$

Finally, for the received signal tensor $\mathcal{X}^{(SR_1R_2D)}$, applying the block-matrix mapping of Section 2, a rank-one approximation to the following fourth-order tensor will be solved at the receiver

$$\mathcal{P}^{(SR_1R_2D)} \approx \mathbf{h}^{(R_2D)} \circ \mathbf{s} \circ \bar{\mathbf{h}}^{(R_1R_2)} \circ \mathbf{h}^{(SR_1)}, \tag{41}$$

with $\mathcal{P}^{(SR_1R_2D)} \in \mathbb{C}^{M_D M_{S_2} \times NR \times M_{S_1} M_{R_2} \times M_{R_1} M_S}$ and $\bar{\mathbf{h}}^{(R_1R_2)} = \mathrm{vec}(\mathbf{H}^{(R_1R_2)\mathrm{T}})$.

4.1. Design requirements

To solve the Kronecker approximation problems (35) and (37), the effective coding matrices $\mathbf{Z}^{(1)}$, $\mathbf{Z}^{(2)}$, $\mathbf{W}_{(3)}^{\mathrm{T}}$ must have full row-rank to be right invertible. As we have discussed before, we choose a semi-unitary design for these matrices, which naturally fulfills such a requirement, while avoiding the calculation of pseudo-inverses. Hence, in terms of system parameter choices, we obtain the following inequalities that have to be satisfied by the proposed design:

$$P \geq F_1 \geq M_S R, \tag{42}$$

$$J \geq F_2 \geq M_{R_1} M_{S_1}, \tag{43}$$

$$K \geq F_3 \geq M_{R_2} M_{S_2}. \tag{44}$$

The proof of (42)–(44) is given in the Appendix C.

5. Proposed semi-blind receivers

In this section, we derive two semi-blind receivers that combine the tensor received signals of the multiple relay links via coupled rank-one tensor approximation problems while exploiting cooperative diversity in different ways. The first algorithm, referred to as coupled-SVD (C-SVD), illustrated in Fig. 3, estimates all the involved communication channels and transmitted symbols in a closed form. The second solution consists of a coupled alternating least squares (C-ALS) algorithm that combines estimates from multiple cooperative links while avoiding matrix inversions due to the rank-one property of the involved signals. Before presenting the proposed receivers, we start with the tensor-based models for the signals received at the destination from the two relays during Phases 2 and 3, respectively. Exploiting the orthogonal PARAFAC decomposition of the space-time coding tensors, we cast joint channel and symbol estimation as coupled rank-one tensor approximation problems.

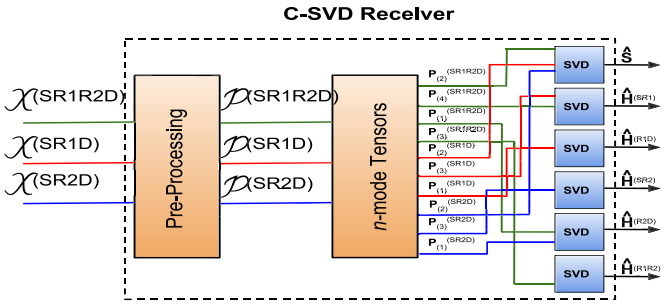

Fig. 3. Block diagram of the C-SVD receiver.

5.1. C-SVD receiver

After the space-time decoding stage, the destination extracts three noisy rank-one tensors given by (39), (40), and (41). In the following, let us recall these three tensors for convenience

$$\mathcal{P}^{(SR_1D)} \approx \mathbf{h}^{(R_1D)} \circ \mathbf{s} \circ \mathbf{h}^{(SR_1)} \tag{45}$$

$$\mathcal{P}^{(SR_2D)} \approx \mathbf{h}^{(R_2D)} \circ \mathbf{s} \circ \mathbf{h}^{(SR_2)} \tag{46}$$

$$\mathcal{P}^{(SR_1R_2D)} \approx \mathbf{h}^{(R_2D)} \circ \mathbf{s} \circ \bar{\mathbf{h}}^{(R_1R_2)} \circ \mathbf{h}^{(SR_1)} \tag{47}$$

The **C**oupled-**SVD** receiver combines these tensor signals to jointly estimate symbols and channels estimation by means of SVDs of appropriate n-mode unfoldings. First, we consider symbol estimation. By coupling the tall 2-mode unfoldings of these tensors, we have

$$\begin{bmatrix} \mathbf{P}_{(2)}^{(SR_1D)\mathrm{T}} \\ \mathbf{P}_{(2)}^{(SR_2D)\mathrm{T}} \\ \mathbf{P}_{(2)}^{(SR_1R_2D)\mathrm{T}} \end{bmatrix} \approx \begin{bmatrix} (\mathbf{h}^{(SR_1)} \otimes \mathbf{h}^{(R_1D)}) \\ (\mathbf{h}^{(SR_2)} \otimes \mathbf{h}^{(R_2D)}) \\ (\mathbf{h}^{(SR_1)} \otimes \bar{\mathbf{h}}^{(R_1R_2)} \otimes \mathbf{h}^{(R_2D)}) \end{bmatrix} \mathbf{s}^{\mathrm{T}}. \tag{48}$$

Eq. (48) is an approximation to a rank-one matrix. Computing the SVD of (48) as $\mathbf{U}_s \mathbf{\Sigma}_s \mathbf{V}_s^{\mathrm{H}}$, the first right singular vector only provide us a basis, i.e., $\hat{\mathbf{s}} = \alpha_1 \mathbf{V}_{s(:,1)}^{*}$, where α_1 is a scalar factor that compensates the orthonormal basis from the SVD. Assuming the knowledge of one symbol, say, $\mathbf{S}_{(1,1)}$, the scalar factor is found as $\alpha_1 = \mathbf{S}_{(1,1)} / \mathbf{V}_{s(1,1)}^{*}$. At the end, the transmitted symbol matrix is obtained by applying the unvec operator, i.e., $\hat{\mathbf{S}} = \mathrm{unvec}(\hat{\mathbf{s}}) \in \mathbb{C}^{N \times R}$.

To estimate the channel $\hat{\mathbf{h}}^{(R_2D)}$, the matrices $\mathbf{P}_{(1)}^{(SR_2D)\mathrm{T}}$ and $\mathbf{P}_{(1)}^{(SR_1R_2D)\mathrm{T}}$, denoting the tall 1-mode unfoldings of the tensors $\mathcal{P}^{(SR_2D)}$ and $\mathcal{P}^{(SR_1R_2D)}$ respectively, are coupled to form another rank-one matrix, as follows

$$\begin{bmatrix} \mathbf{P}_{(1)}^{(SR_2D)\mathrm{T}} \\ \mathbf{P}_{(1)}^{(SR_1R_2D)\mathrm{T}} \end{bmatrix} \approx \begin{bmatrix} (\mathbf{h}^{(SR_2)} \otimes \mathbf{s}) \\ (\mathbf{h}^{(SR_1)} \otimes \bar{\mathbf{h}}^{(R_1R_2)} \otimes \mathbf{s}) \end{bmatrix} \mathbf{h}^{(R_2D)\mathrm{T}}. \tag{49}$$

By computing its SVD as $\mathbf{U}^{(R_2D)} \mathbf{\Sigma}^{(R_2D)} \mathbf{V}^{(R_2D)\mathrm{H}}$, we have that $\hat{\mathbf{H}}^{(R_2D)} = \mathrm{unvec}(\hat{\mathbf{h}}^{(R_2D)}) \in \mathbb{C}^{M_D \times M_{S_2}}$, where $\hat{\mathbf{h}}^{(R_2D)} = \alpha_2 \mathbf{V}_{(:,1)}^{(R_2D)*}$ and $\alpha_2 = \mathbf{H}_{(1,1)}^{(R_2D)} / \mathbf{V}_{(1,1)}^{(R_2D)*}$.

For the estimation of the channel between source and Relay 1, the C-SVD receiver couples the tall 3-mode unfolding of $\mathcal{P}^{(SR_1D)}$ with the tall 4-mode unfolding of $\mathcal{P}^{(SR_1R_2D)}$, yielding another rank-one matrix approximation as

$$\begin{bmatrix} \mathbf{P}_{(3)}^{(SR_1D)\mathrm{T}} \\ \mathbf{P}_{(4)}^{(SR_1R_2D)\mathrm{T}} \end{bmatrix} \approx \begin{bmatrix} (\mathbf{s} \otimes \mathbf{h}^{(R_1D)}) \\ (\bar{\mathbf{h}}^{(R_1R_2)} \otimes \mathbf{s} \otimes \mathbf{h}^{(R_2D)}) \end{bmatrix} \mathbf{h}^{(SR_1)\mathrm{T}}. \tag{50}$$

Computing the SVD of (50) as $\mathbf{U}^{(SR_1)} \mathbf{\Sigma}^{(SR_1)} \mathbf{V}^{(SR_1)\mathrm{H}}$, the channel is estimated as $\hat{\mathbf{h}}^{(SR_1)} = \alpha_3 \mathbf{V}_{(:,1)}^{(SR_1)*}$ with $\alpha_3 = \mathbf{H}_{(1,1)}^{(SR_1)} / \mathbf{V}_{(1,1)}^{(SR_1)*}$. To eliminate the scaling ambiguities in the estimated channels, the knowledge of one entry of each channel matrix suffices. In practice, a

training pilot can be used to estimate the unknown channel coefficient beforehand. However, this training-phase will not be counted in the system transmission rate, due to the fact that the total number of symbol periods needed in this phase is too small compared to the total time redundancy in the proposed system. The same assumption was adopted in Ximenes et al. [22] and Favier et al. [23]. The C-SVD algorithm is summarized in Algorithm 1.

Algorithm 1 C-SVD.

1: **Inputs:** $\mathcal{P}^{(SR_1R_2D)}$, $\mathcal{P}^{(SR_1D)}$ and $\mathcal{P}^{(SR_2D)}$;
2: Estimate the system parameters computing rank-one SVDs and selecting the right dominant singular vector from the following unfoldings:
$\hat{\mathbf{s}}$: from Eq. (48);
$\hat{\mathbf{h}}^{(R_2D)}$: from Eq. (49);
$\hat{\mathbf{h}}^{(SR_1)}$: from Eq. (50);
$\hat{\mathbf{h}}^{(R_1D)}$: using $\mathbf{P}_{(1)}^{(SR_1D)\mathrm{T}}$;
$\hat{\mathbf{h}}^{(SR_2)}$: using $\mathbf{P}_{(3)}^{(SR_2D)\mathrm{T}}$;
$\hat{\bar{\mathbf{h}}}^{(R_1R_2)}$: using $\mathbf{P}_{(3)}^{(SR_1R_2D)\mathrm{T}}$;
3: Apply the unvec operator to recover $\hat{\mathbf{S}}$, $\hat{\mathbf{H}}^{(R_2D)}$, $\hat{\mathbf{H}}^{(S_1R)}$, $\hat{\mathbf{H}}^{(R_1D)}$, $\hat{\mathbf{H}}^{(S_2R)}$ and $\hat{\bar{\mathbf{H}}}^{(R_1R_2)\mathrm{T}}$.
4: Remove the scaling ambiguity according to the knowledge of one element in each system parameter factor matrix.

5.2. C-ALS receiver

The Coupled-ALS receiver is based on the well-known trilinear alternating least squares (ALS) algorithm [36], which provides estimates of the channel and symbol matrices by solving LS problems in an alternating way. Despite its conceptual simplicity, the ALS algorithm may suffer from convergence problems due to its sensitivity to initialization. Moreover, each iteration of trilinear ALS involves three matrix inverses, which can be computationally complex depending on the tensor dimensions. In our context, however, the problem is simpler since we are dealing only with rank-one tensor approximations avoiding the computation of matrix inverses, while yielding fast convergence of the algorithm, which is usually achieved within a few iterations. It is worth mentioning that other algorithms exist in the literature to solve the rank-one tensor approximation problem [33–35].

Using Eqs. (48)–(50), and the unfoldings $\mathbf{P}_{(3)}^{(SR_2D)\mathrm{T}}$, $\mathbf{P}_{(1)}^{(SR_1D)\mathrm{T}}$ and $\mathbf{P}_{(3)}^{(SR_1R_2D)\mathrm{T}}$, the C-ALS receiver solves the following cost functions

$$\hat{\mathbf{s}} = \underset{\mathbf{s}}{\operatorname{argmin}} \left\| \begin{bmatrix} \mathbf{P}_{(2)}^{(SR_1D)\mathrm{T}} \\ \mathbf{P}_{(2)}^{(SR_2D)\mathrm{T}} \\ \mathbf{P}_{(2)}^{(SR_1R_2D)\mathrm{T}} \end{bmatrix} - \begin{bmatrix} \hat{\mathbf{h}}^{(SR_1)} \otimes \hat{\mathbf{h}}^{(R_1D)} \\ \hat{\mathbf{h}}^{(SR_2)} \otimes \hat{\mathbf{h}}^{(R_2D)} \\ \hat{\mathbf{h}}^{(SR_1)} \otimes \hat{\bar{\mathbf{h}}}^{(R_1R_2)} \otimes \hat{\mathbf{h}}^{(R_2D)} \end{bmatrix} \mathbf{s}^{\mathrm{T}} \right\|^2 \tag{51}$$

$$\hat{\mathbf{h}}^{(R_2D)} = \underset{\mathbf{h}^{(R_2D)}}{\operatorname{argmin}} \left\| \begin{bmatrix} \mathbf{P}_{(1)}^{(SR_2D)\mathrm{T}} \\ \mathbf{P}_{(1)}^{(SR_1R_2D)\mathrm{T}} \end{bmatrix} - \begin{bmatrix} \hat{\mathbf{h}}^{(SR_2)} \otimes \hat{\mathbf{s}} \\ \hat{\mathbf{h}}^{(SR_1)} \otimes \hat{\bar{\mathbf{h}}}^{(R_1R_2)} \otimes \hat{\mathbf{s}} \end{bmatrix} \mathbf{h}^{(R_2D)\mathrm{T}} \right\|^2 \tag{52}$$

$$\hat{\mathbf{h}}^{(SR_1)} = \underset{\mathbf{h}^{(R_2D)}}{\operatorname{argmin}} \left\| \begin{bmatrix} \mathbf{P}_{(3)}^{(SR_1D)\mathrm{T}} \\ \mathbf{P}_{(4)}^{(SR_1R_2D)\mathrm{T}} \end{bmatrix} - \begin{bmatrix} \hat{\mathbf{s}} \otimes \hat{\mathbf{h}}^{(R_1D)} \\ \hat{\bar{\mathbf{h}}}^{(R_1R_2)} \otimes \hat{\mathbf{s}} \otimes \hat{\mathbf{h}}^{(R_2D)} \end{bmatrix} \mathbf{h}^{(SR_1)\mathrm{T}} \right\|^2 \tag{53}$$

$$\hat{\mathbf{h}}^{(SR_2)} = \underset{\mathbf{h}^{(SR_2)}}{\operatorname{argmin}} \left\| \mathbf{P}_{(3)}^{(SR_2D)\mathrm{T}} - (\hat{\mathbf{s}} \otimes \hat{\mathbf{h}}^{(R_2D)}) \mathbf{h}^{(SR_2)\mathrm{T}} \right\|^2 \tag{54}$$

$$\hat{\mathbf{h}}^{(R_1D)} = \underset{\mathbf{h}^{(R_1D)}}{\operatorname{argmin}} \left\| \mathbf{P}_{(1)}^{(SR_1D)\mathrm{T}} - (\hat{\mathbf{h}}^{(SR_1)} \otimes \hat{\mathbf{s}}) \mathbf{h}^{(R_1D)\mathrm{T}} \right\|^2 \tag{55}$$

$$\hat{\bar{\mathbf{h}}}^{(R_1R_2)} = \underset{\bar{\mathbf{h}}^{(R_1R_2)}}{\operatorname{argmin}} \left\| \mathbf{P}_{(3)}^{(SR_1R_2D)\mathrm{T}} - (\hat{\mathbf{h}}^{(SR_1)} \otimes \hat{\mathbf{s}} \otimes \hat{\mathbf{h}}^{(R_2D)}) \bar{\mathbf{h}}^{(R_1R_2)\mathrm{T}} \right\|^2 \tag{56}$$

The solutions of Eqs. (51)–(56) are given by

$$\hat{\mathbf{s}} = \frac{1}{3} \begin{bmatrix} \mathbf{P}_{(2)}^{(SR_1D)} & \mathbf{P}_{(2)}^{(SR_2D)} & \mathbf{P}_{(2)}^{(SR_1R_2D)} \end{bmatrix} \begin{bmatrix} \frac{\left(\hat{\mathbf{h}}^{(SR_1)} \otimes \hat{\mathbf{h}}^{(R_1D)}\right)^*}{||\hat{\mathbf{h}}^{(SR_1)}||_2^2 \cdot ||\hat{\mathbf{h}}^{(R_1D)}||_2^2} \\ \frac{\left(\hat{\mathbf{h}}^{(SR_2)} \otimes \hat{\mathbf{h}}^{(R_2D)}\right)^*}{||\hat{\mathbf{h}}^{(SR_2)}||_2^2 \cdot ||\hat{\mathbf{h}}^{(R_2D)}||_2^2} \\ \frac{\left(\hat{\mathbf{h}}^{(SR_1)} \otimes \hat{\bar{\mathbf{h}}}^{(R_1R_2)} \otimes \hat{\mathbf{h}}^{(R_2D)}\right)^*}{||\hat{\mathbf{h}}^{(SR_1)}||_2^2 ||\hat{\bar{\mathbf{h}}}^{(R_1R_2)}||_2^2 ||\hat{\mathbf{h}}^{(R_2D)}||_2^2} \end{bmatrix}, \tag{57}$$

$$\hat{\mathbf{h}}^{(R_2D)} = \frac{1}{2} \begin{bmatrix} \mathbf{P}_{(1)}^{(SR_2D)} & \mathbf{P}_{(1)}^{(SR_1R_2D)} \end{bmatrix} \begin{bmatrix} \frac{\left(\hat{\mathbf{h}}^{(SR_2)} \otimes \hat{\mathbf{s}}\right)^*}{||\hat{\mathbf{h}}^{(SR_2)}||_2^2 \cdot ||\hat{\mathbf{s}}||_2^2} \\ \frac{\left(\hat{\mathbf{h}}^{(SR_1)} \otimes \hat{\bar{\mathbf{h}}}^{(R_1R_2)} \otimes \hat{\mathbf{s}}\right)^*}{||\hat{\mathbf{h}}^{(SR_2)}||_2^2 \cdot ||\hat{\bar{\mathbf{h}}}^{(R_1R_2)}||_2^2 ||\hat{\mathbf{s}}||_2^2} \end{bmatrix}, \tag{58}$$

$$\hat{\mathbf{h}}^{(SR_1)} = \frac{1}{2} \begin{bmatrix} \mathbf{P}_{(3)}^{(SR_1D)} & \mathbf{P}_{(4)}^{(SR_1R_2D)} \end{bmatrix} \begin{bmatrix} \frac{\left(\hat{\mathbf{s}} \otimes \hat{\mathbf{h}}^{(R_1D)}\right)^*}{||\hat{\mathbf{s}}||_2^2 \cdot ||\hat{\mathbf{h}}^{(R_1D)}||_2^2} \\ \frac{\left(\hat{\bar{\mathbf{h}}}^{(R_1R_2)} \otimes \hat{\mathbf{s}} \otimes \hat{\mathbf{h}}^{(R_2D)}\right)^*}{||\hat{\bar{\mathbf{h}}}^{(R_1R_2)}||_2^2 \cdot ||\hat{\mathbf{s}}||_2^2 \cdot ||\hat{\mathbf{h}}^{(R_2D)}||_2^2} \end{bmatrix}, \tag{59}$$

$$\hat{\mathbf{h}}^{(SR_2)} = \mathbf{P}_{(3)}^{(SR_2D)} \left(\frac{(\hat{\mathbf{s}} \otimes \hat{\mathbf{h}}^{(R_2D)})^*}{||\hat{\mathbf{s}}||_2^2 \cdot ||\hat{\mathbf{h}}^{(R_2D)}||_2^2} \right), \tag{60}$$

$$\hat{\mathbf{h}}^{(R_1D)} = \mathbf{P}_{(1)}^{(SR_1D)} \left(\frac{(\hat{\mathbf{h}}^{(SR_1)} \otimes \hat{\mathbf{s}})^*}{||\hat{\mathbf{h}}^{(SR_1)}||_2^2 \cdot ||\hat{\mathbf{s}}||_2^2} \right), \tag{61}$$

$$\hat{\bar{\mathbf{h}}}^{(R_1R_2)} = \mathbf{P}_{(3)}^{(SR_1R_2D)} \left(\frac{(\hat{\mathbf{h}}^{(SR_1)} \otimes \hat{\mathbf{s}} \otimes \hat{\mathbf{h}}^{(R_2D)})^*}{||\hat{\mathbf{h}}^{(SR_1)}||_2^2 \cdot ||\hat{\mathbf{s}}||_2^2 \cdot ||\hat{\mathbf{h}}^{(R_2D)}||_2^2} \right). \tag{62}$$

From steps (57)–(62) the process is repeated until convergence is achieved. The relative error at the end of the ith C-ALS iteration is given by

$$e_i = \frac{||\hat{\mathbf{P}}_i - \mathbf{P}||_F^2}{||\mathbf{P}||_F^2}, \tag{63}$$

where $\mathbf{P}$ is the block matrix that concatenates column-wise the three unfoldings $\mathbf{P}_{(2)}^{(SR_1D)}$, $\mathbf{P}_{(2)}^{(SR_2D)}$, and $\mathbf{P}_{(2)}^{(SR_1R_2D)}$, while $\hat{\mathbf{P}}$ is its reconstructed version from the estimated channels and symbols. The convergence at the ith iteration is declared when $|e_{i-1} - e_i| \leq 10^{-6}$. The C-ALS algorithm is summarized in Algorithm 2.

6. Simulation results

In this section, we evaluate the performance of the C-SVD and the C-ALS receiver in terms of symbol error rate (SER), throughput, normalized mean square error (NMSE) for channel estimation, and computational complexity. The results are averaged over L = 10^4 Monte Carlo runs and each run corresponding to an independent realization of the channels, symbols, and noise. The channel matrices are assumed to have i.i.d. complex Gaussian entries with zero-mean and unitary variance, except for the simulation results of Section 6.5, where the average channel power is varied to consider the effect of path loss on the cooperative links.

Otherwise stated, 64-QAM signals are assumed and the transmitted symbols are normalized at each Monte Carlo run to unity

Algorithm 2 C-ALS.

1: Initialize randomly $\hat{\mathbf{h}}_0^{(R_2D)}$, $\hat{\mathbf{h}}_0^{(SR_1)}$, $\hat{\mathbf{h}}_0^{(SR_2)}$, $\hat{\mathbf{h}}_0^{(R_1D)}$ and $\hat{\mathbf{h}}_0^{(R_1R_2)}$; it = 0;
2: it = it + 1;
3: Calculate the estimate for:
$\hat{\mathbf{s}}_{it}$ using Eq. (57)
$\hat{\mathbf{h}}_{it}^{(R_2D)}$ using Eq. (58)
$\hat{\mathbf{h}}_{it}^{(SR_1)}$ using Eq. (59)
$\hat{\mathbf{h}}_{it}^{(SR_2)}$ using Eq. (60)
$\hat{\mathbf{h}}_{it}^{(R_1D)}$ using Eq. (61)
$\hat{\mathbf{h}}_{it}^{(R_1R_2)}$ using Eq. (62)
4: Return to step 2 and repeat until convergence;
5: Apply the unvec operator to recover $\hat{\mathbf{S}}$, $\hat{\mathbf{H}}^{(R_1D)}$, $\hat{\mathbf{H}}^{(R_2D)}$, $\hat{\mathbf{H}}^{(SR_1)}$, $\hat{\mathbf{H}}^{(SR_2)}$ and $\hat{\mathbf{H}}^{(R_1R_2)}$.

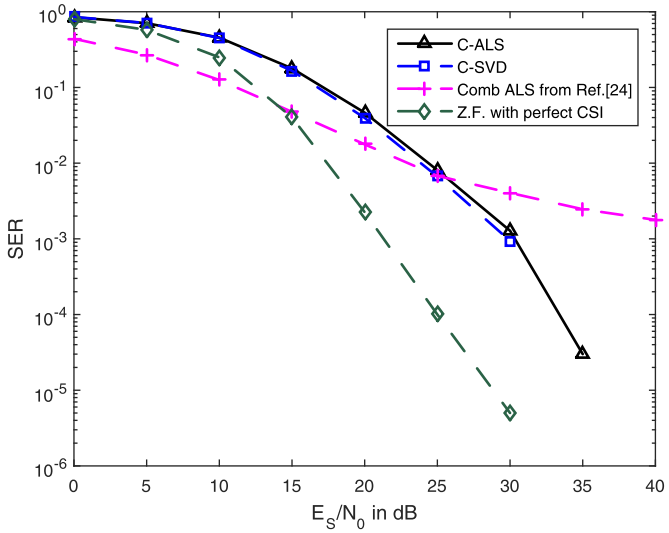

Fig. 4. Proposed receivers vs the iterative proposed in [24].

symbol energy ($E_s = 1$) for each data stream, i.e., $\mathbb{E}\left[\mathbf{S}^{\mathrm{H}}\mathbf{S}\right] = N\mathbf{I}_R$. The SER, throughput, and NMSE curves are plotted as a function of the average E_S/N_0. At each run, the E_S/N_0 ratio is set by controlling the noise variance at the relays and the destination (assumed to be equal). The coding tensors $\mathcal{C}$, $\mathcal{W}$ and $\mathcal{T}$ are normalized by the factors $1/\sqrt{F_1 RM_S}$, $1/\sqrt{F_2 M_{R_1} M_{S_1}}$ and $1/\sqrt{F_3 M_{R_2} M_{S_2}}$, respectively, to ensure that for $P = RM_S$, $J = M_{S_1}M_{R_1}$ and $K = M_{S_2}M_{R_2}$, the coding tensors do not provide any power enhancement. Note that, with this normalization, for $P > RM_S$, $J > M_{R_1}M_{S_1}$ and $K > M_{R_2}M_{S_2}$, the effective coding matrices satisfy $\mathbf{Z}^{(i)}\mathbf{Z}^{(i)\mathrm{H}} = \beta\mathbf{I}$, where $\sqrt{\beta}$ is the power enhancement factor, with $i = \{1, 2\}$.

6.1. Symbol error rate performance

We first evaluate the receivers' performance in terms of their symbol error rate and compare with the one presented in [24]. The simulated scenario is the following: $N = 10$, $R = 2$, $M_S = 2$, $M_D = 4, P = 4$, $J = K = 2$, $M_{S_1} = M_{S_2} = 1$, $M_{R_1} = M_{R_2} = 2$, and $F_1 = RM_S$, $F_2 = M_{R_1}M_{S_1}$, $F_3 = M_{R_2}M_{S_2}$. For the system in [24], a 4-QAM constellation is considered, the number of pilot symbols per time-slot is $N_p = 4$ and the number of time-slots $K = 10$. The parameters were chosen properly to ensure that both systems have the same spectral efficiency. Also, in order to have a reference, we simulate a Zero-Forcing (ZF) receiver with perfect CSI, using Eq. (51). Fig. 4 shows that by comparing the C-SVD with the C-ALS, the performance is almost the same. However, comparing with the system

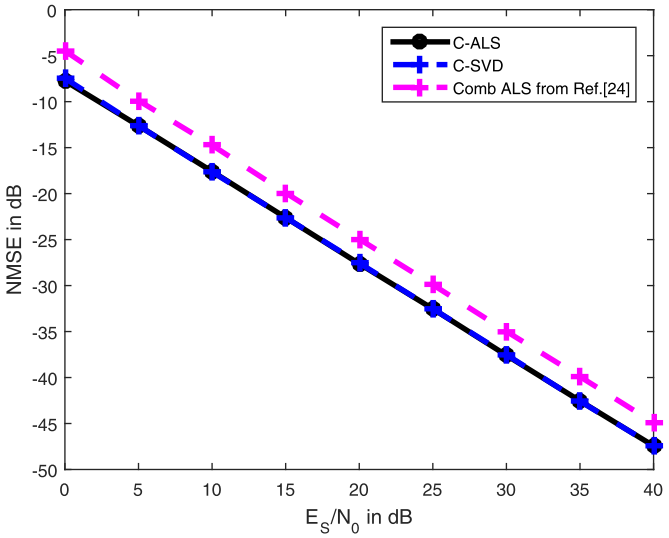

Fig. 5. Normalized mean square error of the system effective channel.

in [24], our proposed receivers show a remarkable gain over the Comb-ALS. This is due the fact that the proposed approach exploits the space-time diversity using space-time coding tensors at the source and relay, while the system in [24] is a supervised one with a long pilot sequence and does not apply any space-time coding at the source. In addition to this performance gain, since our proposed receivers are based on Nested Tucker models, they can exploit a more flexible system design than the ones proposed in Ximenes et al. [22] and Cavalcante et al. [24], which are based on the Nested PARAFAC and PARATUCK-2 models, respectively. More specifically, the proposed receivers can operate with relay stations having different numbers of transmit and receive antennas, in contrast to the ones in Ximenes et al. [22] and Cavalcante et al. [24]. Such a design flexibility is crucial since we can properly choose the number of transmit and receive antennas at the relays to fulfill the design requirements in (43) and (44) using small code lengths (J and K).

6.2. Channel estimation performance

The NMSE is given as

$$\mathrm{NMSE} = \frac{1}{L}\sum_{l=1}^{L}\frac{||\mathbf{H}_{(l)} - \hat{\mathbf{H}}_{(l)}||_F^2}{||\mathbf{H}_{(l)}||_F^2}, \tag{64}$$

where $\mathbf{H}$ represents all channel matrices: $\mathbf{H}^{(SR)}$, $\mathbf{H}^{(RR)}$ and $\mathbf{H}^{(RD)}$, and L is the total number of Monte Carlo realizations. In order to compare with the system in [24], we compute, in Fig. 5, the NMSE of the effective estimated MIMO channel without tensor space-time coding (for this scenario, $M_{S_1} = M_{S_2} = 2$ and $J = K = 4$), which is given by:

$$\begin{bmatrix}\mathbf{X}^{(SR_1D)}\\ \mathbf{X}^{(SR_2D)}\\ \mathbf{X}^{(SR_1R_2D)}\end{bmatrix} = \underbrace{\begin{bmatrix}\hat{\mathbf{H}}^{(R_1D)}\hat{\mathbf{H}}^{(SR_1)}\\ \hat{\mathbf{H}}^{(R_2D)}\hat{\mathbf{H}}^{(SR_2)}\\ \hat{\mathbf{H}}^{(R_2D)}\hat{\mathbf{H}}^{(R_1R_2)}\hat{\mathbf{H}}^{(SR_1)}\end{bmatrix}}_{\mathbf{H}_{\mathrm{eff.}}}\mathbf{S}^{\mathrm{T}}. \tag{65}$$

It can be observed that our rank-one receivers provide a performance gain over the one proposed in [24]. This can be attributed to the fact that the proposed solution has an efficient noise suppression, due to the pre-processing stage and coupled rank-one approach. In Fig. 6, we present the individual channel NMSE performance of the proposed C-SVD and C-ALS receivers. It can be noticed that the relay-destination channels are estimated with higher

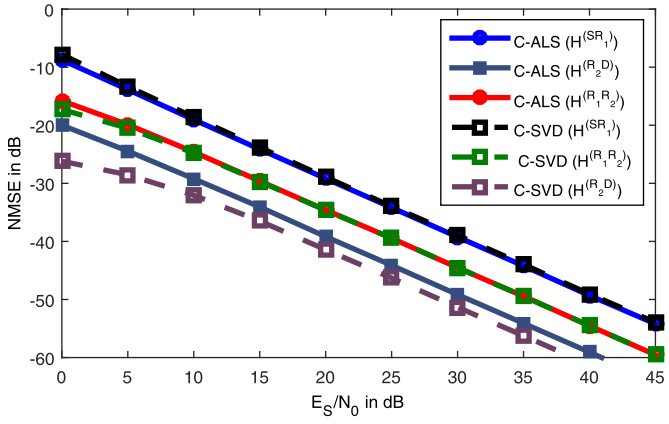

Fig. 6. Normalized mean square error of estimated channels.

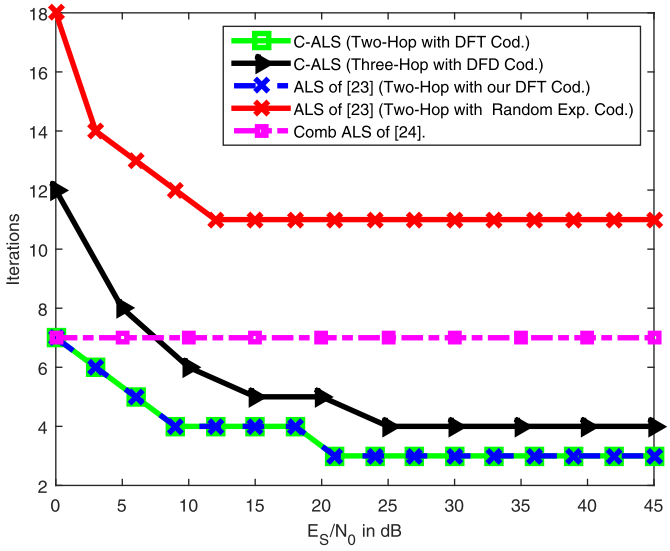

Fig. 7. ALS iterations for convergence.

accuracy than the relay-relay channel and source-relay channels, as expected. Such results can be explained by the fact the for relay-destination channels the signal has already be encoded by three space-time coding tensors, for relay-relay channels, the signal was encoded by two tensors, and for source-relay channels, the signal was encoded only at the source. Comparing the proposed receivers, starting from the source-relay channel estimation, which is the same for both, it can be noticed that for relay-relay and relay-destination channels, the C-SVD receiver offers a small gain in performance over the C-ALS receiver.

6.3. ALS iterations

In Fig. 7, we plot the total number of iterations required for the convergence of the C-ALS receiver. As a reference for comparisons, we also plot the convergence of the Nested-Tucker based ALS receiver of Favier et al. [23], which solves the same problem but using a different tensor model. Therein, the authors also proposed a random exponential design for the space-time coding tensors, while our approach assumes the proposed orthogonal tensor code design based on a exact Khatri-Rao factorization of the DFT matrix. We can observe that the proposed tensor code design results in a significantly lower number of iterations required for convergence, corroborating the importance of the tensor code structure at the receiver.

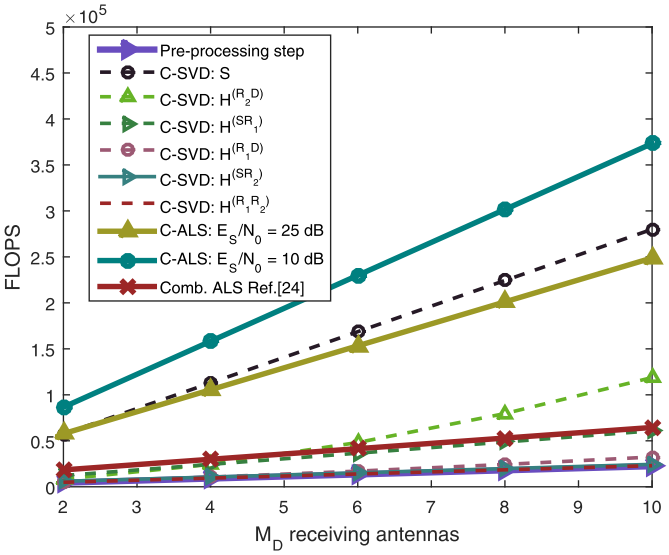

Fig. 8. Number of FLOPS varying the M_D receiving antennas.

6.4. Computational complexity

In this experiment we evaluate the computational complexity of each semi-blind receiver, in terms of floating-point operations per second (FLOPS). Given matrices $\mathbf{A} \in \mathbb{C}^{m\times n}$ and $\mathbf{B} \in \mathbb{C}^{n\times p}$, the number of FLOPS associated with the multiplication of these two matrices is given by $\mathcal{O}(4(mnp))$ (neglecting the additions). For the Kronecker product, the total FLOPS is $\mathcal{O}(4(mn^2p))$, while for the computation of the largest singular value and largest eigenvector we opt for the Power Method approach instead of computing the SVD of a rank-one matrix, for being a cheap choice in terms of computational complexity (see [37]). The Power Method leads to a cost of $I(n^2m + n^2)$ (neglecting the additions and vector normalization) FLOPS, where I is the number of iterations of the Power Method, in which, in our case, for dealing with approximately rank-one matrices, $I = 1$. We compare our proposed receivers with the one in [24]. We can observe in Fig. 8, that the receiver in [24] needs less computational effort than the ours. However, in terms of performance (SER and NMSE) a significant performance gain over the receiver in [24] can be observed in Figs. 4 and 5. Comparing the C-SVD and C-ALS, the first can benefit from a parallel computation, as shown in Fig. 3, while the second one is more attractive at higher E_S/N_0 values, due to the smaller number of iterations required for convergence (Fig. 7).

6.5. Throughput performance

In a final experiment, we study the performance of the C-SVD receiver in terms of throughput computed in bits per channel use, which is the rate of the transmitted information (NR) over the total redundancy in a multi-relaying scenario with a given number of phases. This study provides an insight into the trade-off of the proposed receiver when different modulation and coding schemes are considered. We compare the performance of the proposed three-phases (three-hop) system with a two-phases (two-hop) system (the case where the source is assisted only by Relay 1, i.e., only the signal $\mathcal{X}^{(SR_1D)}$ is considered). In order for both system have the same spectral efficiency, the following parameters were chosen:

- **Three-Phase System**: $N = 10$, $R = 2$, $M_S = 2$, $M_D = 4$, $M_{S_1} = M_{S_2} = 1$, $M_{R_1} = M_{R_2} = 2$ $J = K = 2$ and $P = 4$.
- **Two-Phase System**: $N = 10$, $R = 2$, $M_S = 2$, $M_D = 4$, $M_{R_1} = 4$ $M_{S_1} = 2$, $J = 8$ and $P = 4$.

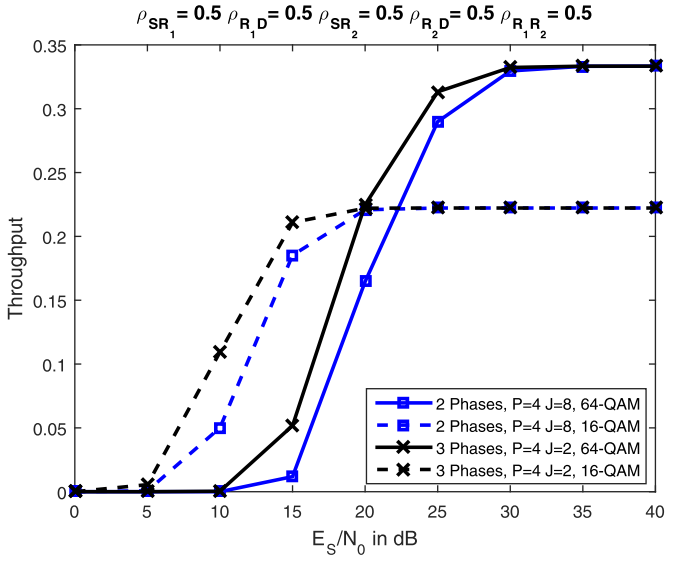

Fig. 9. Throughput for different modulation schemes and code length, P and J values.

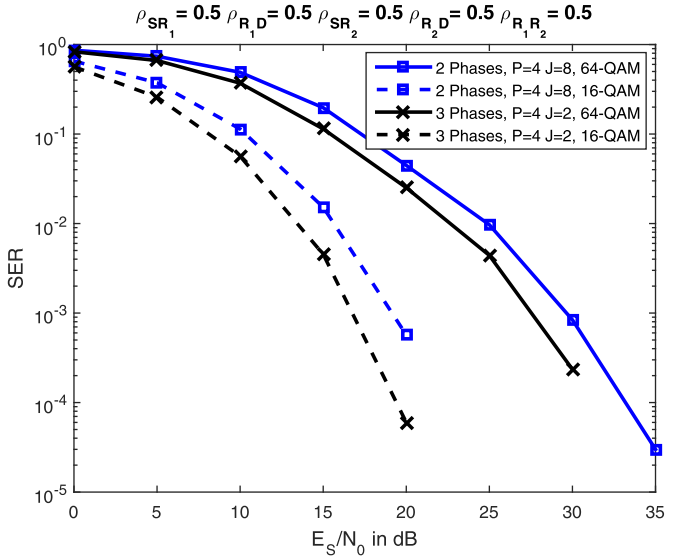

Fig. 10. SER for different modulation schemes and code length, P and J values. P values.

In order to evaluate the performance in a more challenging scenario, we assume spatially correlated channels, by adopting the following the classical model:

$$\mathbf{H} = (\mathbf{R}_{\text{Rx}})^{1/2}\mathbf{H}_w(\mathbf{R}_{\text{Tx}})^{\text{H}/2}, \tag{66}$$

where $\mathbf{R}_{\text{Rx}}$ and $\mathbf{R}_{\text{Tx}}$ are the receive and transmit correlation matrices, respectively and $\mathbf{H}_w$ is a spatially white channel matrix whose coefficients follow a zero-mean circularly-symmetric complex Gaussian distribution. The correlation factor ρ for each channel entry is shown in Figs. 9 and 10.

The throughput is calculated according to the following formula:

$$\text{T} = (1 - \text{PER})\text{T}_{\text{max}}, \tag{67}$$

where PER stands for the packet error rate and T_{max} is the maximum achieved throughput which, for the two- and three-hop systems, are respectively given by

$$\text{T}^{(2)}_{\text{max}} = \frac{R\log_2(M^{(2)})}{P(1+J)}, \tag{68}$$

$$\text{T}^{(3)}_{\text{max}} = \frac{R\log_2(M^{(3)})}{P(1+J+K+JK)}, \tag{69}$$

where $M^{(i)}$ is the number of bits per symbol of the M-QAM constellation used by these systems, $i = 2, 3$. In this work, we adopt the following mapping from BER to PER [38]

$$\text{PER} = 1 - (1 - \text{BER})^{b_l}, \tag{70}$$

where $b_l = N\log_2^{M^{(i)}}$ is the number of bits of a packet. Also, defining d as the distance between the source and destination, we consider the following positioning of the relays

$$\begin{aligned} &d^{(SR_1)} = 0.6d \quad d^{(R_1D)} = 0.5d \\ &d^{(SR_2)} = 0.5d \quad d^{(R_2D)} = 0.6d \quad d^{(R_1R_2)} = 0.6d, \end{aligned} \tag{71}$$

where $d^{(SR_1)}$, $d^{(R_1D)}$, $d^{(SR_2)}$, $d^{(R_2D)}$ and $d^{(R_1R_2)}$ are the distances between the source and Relay 1, Relay 1 and destination, source and Relay 2, Relay 2 and destination, Relay 1 and Relay 2, respectively. The path loss follows the classical model

$$P_R^{(i)} = P_T\left[\frac{d_0^{(i)}}{d}\right]^{\gamma}, \tag{72}$$

where $d_0^{(i)}$ and γ are, respectively, the reference distance for the ith link in (71), and the path loss exponent ($\gamma = 3$), while $P_T = NR$ is the total transmitted signal power. Since the two-hop system only has one relay to assist the source, the modulation scheme and the code length (P, J, or K) are adjusted to ensure that all systems compared have the same rate.

In Fig. 9, it can be noticed that the three-hop system achieves the maximum rate in a lower E_S/N_0 range than the two-hop system, even with the two-hop system having more antennas at the relay station compared to the relays in the three-hop system. The simulation results in Fig. 10, which show the SER performance, corroborate our conclusions in Fig. 9, showing that the proposed three-hop system is more attractive than the two-hop system in this scenario.

7. Conclusions

In this paper, we have proposed two semi-blind receivers for multi-relaying MIMO systems by coupling rank-one tensor approximations problems for multiple cooperative links after space-time combining at the destination. We show that the rank-one approach combined with orthogonal codes provides an excellent performance in comparison with the supervised receiver proposed in [24]. The C-SVD receiver offers closed-form joint channel and symbol estimation that can benefit from parallel processing, being the preferable solution for low signal to noise ratios, while the C-ALS receiver offers a better performance-complexity tradeoff for higher signal to noise ratios. Moreover, our throughput results using different modulation and tensor coding schemes have shown interesting tradeoffs between systems with two and three -hop, for scenarios where the code length of the space-time coding tensors at the relays (J and K) is small. Perspectives of this work include the generalization of the proposed semi-blind receivers to multiuser scenarios, while taking into account more realistic effects such as timing and carrier frequency offsets.

Declaration of Competing Interest

The authors declare that they have no known competing financial interests or personal relationships that could have appeared to influence the work reported in this paper.

Acknowledgment

This work is supported by the National Council for Scientific and Technological Development CNPq Proc. no. 306616/2016-5, CAPES/PROBRAL Proc. no. 88887.144009/2017-00, and CAPES/PRINT Proc. no. 88887.311965/2018-00.

Appendix A. Tensor Coding Design

We propose an orthogonal design for the space-time coding tensors used at the source and relays. The resulting coding structure is exploited in the first step of the proposed semi-blind receiver to decode the received signals at low-complexity, before joint channel and symbol estimation.

First, we impose a PARAFAC structure for each coding tensor used at the source, Relay 1 and Relay 2, as follows

$$\mathcal{C} = \mathcal{I}_{3,F_1} \times_1 \mathbf{C}_1 \times_2 \mathbf{C}_2 \times_3 \mathbf{C}_3 \in \mathbb{C}^{M_S \times R \times P} \tag{A.1}$$

$$\mathcal{W} = \mathcal{I}_{3,F_2} \times_1 \mathbf{W}_1 \times_2 \mathbf{W}_2 \times_3 \mathbf{W}_3 \in \mathbb{C}^{M_{S_1} \times M_{R_1} \times J} \tag{A.2}$$

$$\mathcal{T} = \mathcal{I}_{3,F_3} \times_1 \mathbf{T}_1 \times_2 \mathbf{T}_2 \times_3 \mathbf{T}_3 \in \mathbb{C}^{M_{S_2} \times M_{R_2} \times K}, \tag{A.3}$$

where $\mathbf{C}_1 \in \mathbb{C}^{M_S \times F_1}$, $\mathbf{C}_2 \in \mathbb{C}^{R \times F_1}$, $\mathbf{C}_3 \in \mathbb{C}^{P \times F_1}$, $\mathbf{W}_1 \in \mathbb{C}^{M_{S_1} \times F_2}$, $\mathbf{W}_2 \in \mathbb{C}^{M_{R_1} \times F_2}$, $\mathbf{W}_3 \in \mathbb{C}^{J \times F_2}$, $\mathbf{T}_1 \in \mathbb{C}^{M_{S_2} \times F_3}$, $\mathbf{T}_2 \in \mathbb{C}^{M_{R_2} \times F_3}$ and $\mathbf{T}_3 \in \mathbb{C}^{K \times F_3}$ are the factor matrices of the tensors $\mathcal{C}$, $\mathcal{W}$ and $\mathcal{T}$ respectively.

In order to simplify the notation, we define $\mathbf{z}_{jp}^{(1)}$ and $\mathbf{z}_{kp}^{(2)}$ as the effective coding vectors

$$\mathbf{z}_{jp}^{(1)} = \text{vec}(\mathbf{C}_{..p}^{\text{T}} \otimes \mathbf{W}_{..j}), \in \mathbb{C}^{M_{S_1} R M_{R_1} M_S \times 1} \tag{A.4}$$

$$\mathbf{z}_{kp}^{(2)} = \text{vec}(\mathbf{C}_{..p}^{\text{T}} \otimes \mathbf{T}_{..k}) \in \mathbb{C}^{M_{S_2} R M_{R_2} M_S \times 1}. \tag{A.5}$$

Since the only difference between $\mathbf{z}_{jp}^{(1)}$ and $\mathbf{z}_{kp}^{(2)}$ is the space-time coding tensor at the relays, and noting that these tensors both have a PARAFAC structure, we can apply Properties (1), (2), (3) and (4) in Eq. (A.4), yielding

$$\mathbf{z}_{jp}^{(1)} = \text{vec}(\mathbf{C}_2 \text{D}_p(\mathbf{C}_3) \mathbf{C}_1^{\text{T}} \otimes \mathbf{W}_1 \text{D}_j(\mathbf{W}_3) \mathbf{W}_2^{\text{T}}) \tag{A.6}$$

$$= \text{vec}[(\mathbf{C}_2 \otimes \mathbf{W}_1)(\text{D}_p(\mathbf{C}_3) \otimes \text{D}_j(\mathbf{W}_3))(\mathbf{C}_1 \otimes \mathbf{W}_2)^{\text{T}}] \tag{A.7}$$

$$= [(\mathbf{C}_1 \otimes \mathbf{W}_2) \diamond (\mathbf{C}_2 \otimes \mathbf{W}_1)](\mathbf{C}_{3_p} \otimes \mathbf{W}_{3_j})^{\text{T}}, \tag{A.8}$$

where $\mathbf{C}_{3_p}$ and $\mathbf{W}_{3_j}$ are pth and jth row from $\mathbf{C}_3$ and $\mathbf{W}_3$, respectively. By stacking the JP vectors as columns of $\mathbf{Z}^{(1)} \in \mathbb{C}^{M_{S_1} R M_{R_1} M_S \times JP}$, and defining $\mathbf{G}_1 = (\mathbf{C}_2 \otimes \mathbf{W}_1) \in \mathbb{C}^{M_{S_1} R \times F_2 F_1}$, $\mathbf{G}_2 = (\mathbf{C}_1 \otimes \mathbf{W}_2) \in \mathbb{C}^{M_{R_1} M_S \times F_2 F_1}$, $\mathbf{G}_3 = (\mathbf{C}_3 \otimes \mathbf{W}_3) \in \mathbb{C}^{JP \times F_2 F_1}$, we have

$$\begin{aligned} \mathbf{Z}^{(1)} &= [\mathbf{z}_{1,1}^{(1)}, \ldots, \mathbf{z}_{J,1}^{(1)}, \ldots, \mathbf{z}_{J,P}^{(1)}] \\ &= (\mathbf{G}_2 \diamond \mathbf{G}_1)\mathbf{G}_3^{\text{T}}. \end{aligned} \tag{A.9}$$

In the same way we can apply the steps in (A.6)–(A.8) to Eq. (A.5) and derive the matrix $\mathbf{Z}^{(2)} \in \mathbb{C}^{M_{S_2} R M_{R_2} M_S \times KP}$

$$\begin{aligned} \mathbf{Z}^{(2)} &= [\mathbf{z}_{1,1}^{(2)}, \ldots, \mathbf{z}_{K,1}^{(2)}, \ldots, \mathbf{z}_{K,P}^{(2)}] \\ &= (\mathbf{B}_2 \diamond \mathbf{B}_1)\mathbf{B}_3^{\text{T}}, \end{aligned} \tag{A.10}$$

where $\mathbf{B}_1 = (\mathbf{C}_2 \otimes \mathbf{T}_1) \in \mathbb{C}^{M_{S_2} R \times F_3 F1}$, $\mathbf{B}_2 = (\mathbf{C}_1 \otimes \mathbf{T}_2) \in \mathbb{C}^{M_{R_2} M_S \times F_3 F1}$ and $\mathbf{B}_3 = (\mathbf{C}_3 \otimes \mathbf{T}_3) \in \mathbb{C}^{KP \times F_3 F1}$.

From (A.9) and (A.10), it is clear that the space-time filters $\mathbf{Z}^{(1)}$ and $\mathbf{Z}^{(2)}$ have a PARAFAC structure. Such a structure is exploited to ensure $\mathbf{Z}^{(1)}$ and $\mathbf{Z}^{(2)}$ are semi-unitary, so that the macthed filtering steps (36) and (38) can be applied. The semi-unitary property of the space-time filters is proved in Appendix B.

Appendix B. Proof of the Semi-unitary Property

As previously defined in Appendix A, let us consider the factor matrices of the coding tensors $\mathbf{C}_1 \in \mathbb{C}^{M_S \times F_1}$, $\mathbf{C}_2 \in \mathbb{C}^{R \times F_1}$, $\mathbf{C}_3 \in \mathbb{C}^{P \times F_1}$, $\mathbf{W}_1 \in \mathbb{C}^{M_{S_1} \times F_2}$, $\mathbf{W}_2 \in \mathbb{C}^{M_{R_1} \times F_2}$, $\mathbf{W}_3 \in \mathbb{C}^{J \times F_2}$, $\mathbf{T}_1 \in \mathbb{C}^{M_{S_2} \times F_3}$, $\mathbf{T}_2 \in \mathbb{C}^{M_{R_2} \times F_3}$ and $\mathbf{T}_3 \in \mathbb{C}^{K \times F_3}$. Given the PARAFAC structures for $\mathbf{Z}^{(1)}$ and $\mathbf{Z}^{(2)}$ in Eq. (A.9) and (A.10) respectively, our goal is to design these factor matrices such that $\mathbf{Z}^{(1)}\mathbf{Z}^{(1)\text{H}} = \mathbf{I}_{M_{S_1} R M_{R_1} M_S}$ and $\mathbf{Z}^{(2)}\mathbf{Z}^{(2)\text{H}} = \mathbf{I}_{M_{S_2} R M_{R_2} M_S}$. Let us take $\mathbf{Z}^{(1)}$ as an example, and define the matrix $\mathbf{Z}_P^{(1)} \in \mathbb{C}^{M_{S_1} M_{R_1} M_S R \times JP}$ as

$$\begin{aligned} \mathbf{Z}_P^{(1)} &= \mathbf{\Pi}\mathbf{Z}^{(1)} \\ &= \mathbf{\Pi}[(\mathbf{C}_1 \otimes \mathbf{W}_2) \diamond (\mathbf{C}_2 \otimes \mathbf{W}_1)](\mathbf{C}_3 \otimes \mathbf{W}_3)^{\text{T}} \\ &= [(\mathbf{C}_2 \diamond \mathbf{C}_1) \otimes (\mathbf{W}_2 \diamond \mathbf{W}_1)](\mathbf{C}_3 \otimes \mathbf{W}_3)^{\text{T}}, \end{aligned} \tag{B.1}$$

where $\mathbf{\Pi}$ is a permutation matrix that exchanges the rows of $\mathbf{Z}^{(1)}$ in order to obtain Eq. (B.1). Note that if $\mathbf{Z}_P^{(1)}$ has orthogonal rows, then $\mathbf{Z}^{(1)}$ would also have orthogonal rows, since a permutation matrix is orthogonal. Defining as $\overline{\mathbf{C}} = \mathbf{C}_2 \diamond \mathbf{C}_1 \in \mathbb{C}^{M_S R \times F_1}$ and $\overline{\mathbf{W}} = \mathbf{W}_2 \diamond \mathbf{W}_1 \in \mathbb{C}^{M_{S_1} M_{R_1} \times F_2}$, and replacing them in Eq. (B.1), we have

$$\mathbf{Z}_P^{(1)}\mathbf{Z}_P^{(1)\text{H}} = (\overline{\mathbf{C}} \otimes \overline{\mathbf{W}})\mathbf{G}_3^{\text{T}}\mathbf{G}_3^{*}(\overline{\mathbf{C}} \otimes \overline{\mathbf{W}})^{\text{H}}. \tag{B.2}$$

Noting that $\mathbf{G}_3 = \mathbf{C}_3 \otimes \mathbf{W}_3$, and choosing $\mathbf{C}_3$ and $\mathbf{W}_3$ as DFT matrices (assuming $P = F_1$ and $J = F_2$), we have:

$$\begin{aligned} \mathbf{G}_3^{\text{T}}\mathbf{G}_3^{*} &= \frac{1}{F_1 F_2}(\mathbf{C}_3 \otimes \mathbf{W}_3)^{\text{T}}(\mathbf{C}_3 \otimes \mathbf{W}_3)^{*} \\ &= \frac{1}{F_1 F_2}(\mathbf{C}_3^{\text{T}}\mathbf{C}_3^{*} \otimes \mathbf{W}_3^{\text{T}}\mathbf{W}_3^{*}) \\ &= \mathbf{I}_{F_1 F_2}, \end{aligned}$$

where $\frac{1}{\sqrt{F_1 F_2}}$ is the normalization factor for the DFTs matrices. The condition $\mathbf{Z}_P^{(1)}\mathbf{Z}_P^{(1)\text{H}} = \mathbf{I}_{M_{S_1} R M_{R_1} M_S}$ is now dependent on the choice of $\overline{\mathbf{C}} \in \mathbb{C}^{F_1 \times F_1}$ and $\overline{\mathbf{W}} \in \mathbb{C}^{F_2 \times F_2}$. Choosing a DFT structure for these matrices implies

$$\begin{aligned} \mathbf{Z}_P^{(1)}\mathbf{Z}_P^{(1)\text{H}} &= \frac{1}{R M_S M_{R_1} M_{S_1}}(\overline{\mathbf{C}}\overline{\mathbf{C}}^{\text{H}}) \otimes (\overline{\mathbf{W}}\overline{\mathbf{W}}^{\text{H}}) \\ &= \mathbf{I}_{R M_S M_{R_1} M_{S_1}}. \end{aligned} \tag{B.3}$$

Since each column of the DFT matrix is a Vandermonde vector, it turns out that $\overline{\mathbf{C}}$ and $\overline{\mathbf{W}}$ can be factorized exactly as the Khatri-Rao product of two or more lower-dimensional matrices. As example, consider the DFT structure for $\overline{\mathbf{C}}$ as

$$\overline{\mathbf{C}} = \frac{1}{\sqrt{F_1}}\begin{bmatrix} 1 & 1 & 1 & \cdots & 1 \\ 1 & \omega & \omega^2 & \cdots & \omega^{F_1-1} \\ 1 & \omega^2 & \omega^4 & \cdots & \omega^{2(F_1-1)} \\ \vdots & \vdots & \vdots & \cdots & \vdots \\ 1 & \omega^{F_1-1} & \omega^{2(F_1-1)} & \cdots & \omega^{(F_1-1)(F_1-1)} \end{bmatrix},$$

where $\omega = e^{-2j\pi/F_1}$. The (f_1+1)th column of $\overline{\mathbf{C}}$ can be decomposed as:

$$\overline{\mathbf{c}}_{f_1+1} = \begin{bmatrix} 1 \\ \omega \\ \omega^2 \\ \vdots \\ \omega^{f_1(R-1)} \end{bmatrix}^{M_S} \otimes \begin{bmatrix} 1 \\ \omega \\ \omega^2 \\ \vdots \\ \omega^{f_1(M_S-1)} \end{bmatrix}. \tag{B.4}$$

Therefore, factorizing the F_1 columns of $\overline{\mathbf{C}}$ implies that $\overline{\mathbf{C}} = \mathbf{C}_2 \diamond \mathbf{C}_1$, from which we find $\mathbf{C}_1$ and $\mathbf{C}_2$. The same is valid to find $\mathbf{W}_1$ and $\mathbf{W}_2$ from $\overline{\mathbf{W}}$.

In the same way as for $\mathbf{Z}_P^{(1)}$, we have $\mathbf{Z}_P^{(2)} \in \mathbb{C}^{M_{S_2} M_{R_2} M_S R \times KP}$ defined as

$$\begin{aligned}\mathbf{Z}_P^{(2)} &= \mathbf{\Pi}\mathbf{Z}^{(2)} \\ &= \mathbf{\Pi}[(\mathbf{C}_1 \otimes \mathbf{T}_2) \diamond (\mathbf{C}_2 \otimes \mathbf{T}_1)](\mathbf{C}_3 \otimes \mathbf{T}_3)^{\mathrm{T}} \\ &= [(\mathbf{C}_2 \diamond \mathbf{C}_1) \otimes (\mathbf{T}_2 \diamond \mathbf{T}_1)](\mathbf{C}_3 \otimes \mathbf{T}_3)^{\mathrm{T}}, \end{aligned} \tag{B.5}$$

where $\mathbf{\Pi}$ is a permutation matrix that exchanges the rows of $\mathbf{Z}^{(2)}$ defined in Eq. (A.10). In this case, defining $\overline{\mathbf{T}} = \mathbf{T}_2 \diamond \mathbf{T}_1 \in \mathbb{C}^{M_{R_2} M_{S_2} \times F_3}$ and noting that $\mathbf{B}_3 = \mathbf{C}_3 \otimes \mathbf{T}_3$, we have

$$\mathbf{Z}_P^{(2)} \mathbf{Z}_P^{(2)\mathrm{H}} = (\overline{\mathbf{C}} \otimes \overline{\mathbf{T}}) \mathbf{B}_3^{\mathrm{T}} \mathbf{B}_3^{*} (\overline{\mathbf{C}} \otimes \overline{\mathbf{T}})^{\mathrm{H}}. \tag{B.6}$$

From Eq. (B.6) we can easily see that choosing $\mathbf{T}_3$ and $\overline{\mathbf{T}}$ as DFT matrices, $\mathbf{Z}_P^{(2)}$ has orthogonal rows, i.e., $\mathbf{Z}_P^{(2)} \mathbf{Z}_P^{(2)\mathrm{H}} = \mathbf{I}_{M_{S_2} M_{R_2} M_S R}$, from which we can conclude that $\mathbf{Z}^{(2)} \mathbf{Z}^{(2)\mathrm{H}} = \mathbf{I}_{M_{S_2} R M_{R_2} M_S}$. Applying the factorization (B.4) to the columns of $\overline{\mathbf{T}}$ we get $\mathbf{T}_1$ and $\mathbf{T}_2$. Finally, it remains to prove the semi-unitary property of $\mathbf{W}_{(3)}$, which from Eq. (A.2) is written as

$$\begin{aligned}\mathbf{W}_{(3)}^{\mathrm{T}} &= (\mathbf{W}_2 \diamond \mathbf{W}_1) \mathbf{W}_3^{\mathrm{T}} \\ &= \overline{\mathbf{W}} \mathbf{W}_3^{T}. \end{aligned} \tag{B.7}$$

Since $\overline{\mathbf{W}}$ and $\mathbf{W}_3$ are assumed to be DFT matrices, we have

$$\begin{aligned}\mathbf{W}_{(3)}^{\mathrm{T}} \mathbf{W}_{(3)}^{*} &= \overline{\mathbf{W}} \mathbf{W}_3^{T} \mathbf{W}_3^{*} \overline{\mathbf{W}}^{\mathrm{H}} \\ &= \overline{\mathbf{W}} \mathbf{I}_{F_2} \overline{\mathbf{W}}^{H} \\ &= \mathbf{I}_{M_{S_1} M_{R_1}}, \end{aligned} \tag{B.8}$$

which completes the proof. □

Appendix C. Code Design Requirements

As mentioned in Section 4.1, the matrices $\mathbf{Z}^{(1)}$, $\mathbf{Z}^{(2)}$ and $\mathbf{W}_{(3)}^{\mathrm{T}}$ must have full row-rank to fulfill the semi-unitary property. Let us first recall the following properties

- $\mathrm{rank}(\mathbf{A} \otimes \mathbf{B}) = \mathrm{rank}(\mathbf{A})\mathrm{rank}(\mathbf{B})$
- $\mathrm{rank}(\mathbf{AB}) = \mathrm{rank}(\mathbf{A})$ if $\mathbf{B}$ is a full rank matrix.

The rank of $\mathbf{Z}^{(1)}$ its equal to the rank of $\mathbf{Z}_P^{(1)}$, and is given by

$$\mathrm{rank}(\mathbf{Z}_P^{(1)}) = \mathrm{rank}([\overline{\mathbf{C}} \otimes \overline{\mathbf{W}}] \mathbf{G}_3^{\mathrm{T}}). \tag{C.1}$$

The rank of $\mathbf{G}_3^{\mathrm{T}}$ can be expressed as

$$\begin{aligned}\mathrm{rank}(\mathbf{G}_3^{\mathrm{T}}) &= \mathrm{rank}(\mathbf{C}_3^{\mathrm{T}} \otimes \mathbf{W}_3^{\mathrm{T}}) \\ &= \mathrm{rank}(\mathbf{C}_3^{\mathrm{T}}) \mathrm{rank}(\mathbf{W}_3^{\mathrm{T}}). \end{aligned} \tag{C.2}$$

Since $\mathbf{C}_3$ is of size $P \times F_1$ and $\mathbf{W}_3$ of size $J \times F_2$, for $\mathbf{G}_3^{\mathrm{T}} \in \mathbb{C}^{F_2 F_1 \times JP}$ to have full row-rank matrix, we must have $\mathrm{rank}(\mathbf{C}_3) = F_1$ and $\mathrm{rank}(\mathbf{W}_3) = F_2$, which requires $P \geq F_1$ and $J \geq F_2$. Since the matrix $\mathbf{G}_3^{\mathrm{T}}$ is full row-rank, the rank of $\mathbf{Z}_P^{(1)}$ is given by

$$\begin{aligned}\mathrm{rank}(\mathbf{Z}_P^{(1)}) &= \mathrm{rank}(\overline{\mathbf{C}} \otimes \overline{\mathbf{W}}) \\ &= \mathrm{rank}(\overline{\mathbf{C}}) \mathrm{rank}(\overline{\mathbf{W}}) \\ &= \mathrm{rank}([\mathbf{C}_2 \diamond \mathbf{C}_1]) \mathrm{rank}([\mathbf{W}_2 \diamond \mathbf{W}_1]). \end{aligned} \tag{C.3}$$

For $\mathbf{Z}_P^{(1)}$ to have full row-rank, $\overline{\mathbf{C}} \in \mathbb{C}^{RM_S \times F_1}$ and $\overline{\mathbf{W}} \in \mathbb{C}^{M_{S_1} M_{R_1} \times F_2}$ must also have a full row-rank, which requires $F_1 \geq RM_S$ and $F_2 \geq M_{S_1} M_{R_1}$. Combining these conditions, we arrive at the inequalities given in (42)–(43). Finally, computing the rank of $\mathbf{Z}_P^{(2)}$ defined in (B.5), and using (C.1), we arrive at the condition $K \geq F_3 \geq M_{S_2} M_{R_2}$ given in (44). □

References

[1] Y. Gao, Y. Chen, K.R. Liu, Cooperation stimulation for multiuser cooperative communications using indirect reciprocity game, IEEE Trans. Commun. 60 (12) (2012) 3650–3661.
[2] K. Liu, A. Sadek, W. Su, A. Kwasinski, Cooperative Communications and Networking, Cambridge University Press, 2008.
[3] B. Chen, M. Lei, M. Zhao, An optimal resource allocation method for multi-User multi-Relay DF cognitive radio networks, IEEE Commun. Lett. 20 (6) (2016) 1164–1167.
[4] L. Cao, J. Zhang, N. Kanno, Multi-user cooperative communications with relay–coding for Uplink IMT-advanced 4G systems, in: Proc. IEEE Global Telecommunications Conference (GLOBECOM 2009), 2009, pp. 1–6.
[5] H. Frank, F. Katz, Cooperation in Wireless Networks: Principles and Applications: Real Egoistic Behavior is to Cooperate!, Springer-Verlag New York, Inc., 2006.
[6] M. Dohler, Y. Li, Cooperative Communications: Hardware, Channel and PHY, John Wiley & Sons, 2010.
[7] Y. Rong, Optimal joint source and relay beamforming for MIMO relays with direct link, IEEE Commun. Lett. 14 (5) (2010) 390–392.
[8] T. Liu, S. Zhu, Joint CFO and channel estimation for asynchronous cooperative communication systems, IEEE Signal Process. Lett. 19 (10) (2012) 643–646.
[9] Y. Yao, X. Dong, Multiple CFO mitigation in amplify-and-forward cooperative OFDM transmission, IEEE Trans. Commun. 60 (12) (2012) 3844–3854.
[10] A.L.F. de Almeida, G. Favier, J.C.M. Mota, A constrained factor decomposition with application to MIMO antenna systems, IEEE Trans. Signal Process. 56 (6) (2008) 2429–2442.
[11] G. Favier, M.N. da Costa, A.L.F. de Almeida, J.M.T. Romano, Tensor space–time (TST) coding for MIMO wireless communication systems, Signal Process. 92 (4) (2012) 1079–1092.
[12] A.L.F. de Almeida, G. Favier, Double Khatri–Rao space-time-frequency coding using semi-blind PARAFAC based receiver, IEEE Signal Process. Lett. 20 (5) (2013) 471–474.
[13] K. Liu, J.P.C. da Costa, H. So, A.L.F. de Almeida, Semi-blind receivers for joint symbol and channel estimation in space-time-frequency MIMO-OFDM systems, IEEE Trans. Signal Process. 61 (21) (2013) 5444–5457.
[14] A.L.F. de Almeida, G. Favier, L.R. Ximenes, Space-time-frequency (STF) MIMO communication systems with blind receiver based on a generalized PARATUCK2 model, IEEE Trans. Signal Process. 61 (8) (2013) 1895–1909.
[15] E. Acar, T.G. Kolda, D.M. Dunlavy, All-at-once optimization for coupled matrix and tensor factorizations, arXiv preprint arXiv:1105.3422 (2011).
[16] K.Y. Yılmaz, A.T. Cemgil, U. Simsekli, Generalised coupled tensor factorisation, in: Advances in Neural Information Processing Systems, 2011, pp. 2151–2159.
[17] M. Sørensen, L. De Lathauwer, Coupled tensor decompositions for applications in array signal processing, in: 2013 5th IEEE International Workshop on Computational Advances in Multi-Sensor Adaptive Processing (CAMSAP), IEEE, 2013, pp. 228–231.
[18] F. Roemer, M. Haardt, Tensor-based channel estimation and iterative refinements for two-way relaying with multiple antennas and spatial reuse, IEEE Trans. Signal Process. 58 (11) (2010) 5720–5735.
[19] C.A.R. Fernandes, A.L.F. de Almeida, D.B. da Costa, Unified tensor modeling for blind receivers in multiuser uplink cooperative systems, IEEE Signal Process. Lett. 19 (5) (2012) 247–250.
[20] Y. Rong, M.R.A. Khandaker, Y. Xiang, Channel estimation of dual-hop MIMO relay system via parallel factor analysis, IEEE Trans. Wireless Commun. 11 (6) (2012) 2224–2233.
[21] A.L.F. de Almeida, C.A. Fernandes, D.B. da Costa, Multiuser detection for uplink DS-CDMA amplify-and-Forward relaying systems, IEEE Signal Process. Lett. 20 (7) (2013) 697–700.
[22] L.R. Ximenes, G. Favier, A.L.F. de Almeida, Semi-Blind receivers for non-Regenerative cooperative MIMO communications based on nested PARAFAC modeling, IEEE Trans. Signal Process. 63 (18) (2015) 4985–4998.
[23] G. Favier, C.A.R. Fernandes, A.L.F. de Almeida, Nested tucker tensor decomposition with application to MIMO relay systems using tensor space–Time coding (TSTC), Signal Process. 128 (2016) 318–331.
[24] I.V. Cavalcante, A.L.F. de Almeida, M. Haardt, Tensor-based approach to channel estimation in amplify-and-forward MIMO relaying systems, in: Proc. IEEE 8th Sensor Array and Multichannel Signal Processing Workshop (SAM 2014), 2014, pp. 445–448.
[25] R.A. Harshman, Foundations of the PARAFAC procedure: models and conditions for an "explanatory" multi-modal factor analysis (1970).
[26] L.R. Tucker, Some mathematical notes on three-mode factor analysis, Psychometrika 31 (3) (1966) 279–311.
[27] J. Du, C. Yuan, Z. Hu, H. Lin, A novel tensor-based receiver for joint symbol and channel estimation in two-hop cooperative MIMO relay systems, IEEE Commun. Lett. 19 (11) (2015) 1961–1964.
[28] B. Sokal, A.L.F. de Almeida, M. Haardt, Rank-one tensor modeling approach to joint channel and symbol estimation in two-hop MIMO relaying systems, in: Proc. XXXV Simpósio Brasileiro de Telecomunicações e Processamento de Sinais (SBrT 2017), 2017.
[29] C. Van Loan, N. Pitsianis, Approximation with Kronecker Products, Technical Report, Cornell University, 1992.
[30] K. Naskovska, M. Haardt, A.L.F. de Almeida, Generalized tensor contraction with application to Khatri-Rao coded MIMO OFDM systems, in: Proc. IEEE 7th International Workshop on Computational Advances in Multi-Sensor Adaptive Processing (CAMSAP 2017), 2017, pp. 1–5.

[31] J.G. Nagy, M.E. Kilmer, Kronecker product approximation for preconditioning in three-dimensional imaging applications, IEEE Trans. Image Process. 15 (3) (2006) 604–613.
[32] K.K. Wu, Y. Yam, H. Meng, M. Mesbahi, Kronecker product approximation with multiple factor matrices via the tensor product algorithm, in: Proc. IEEE International Conference on Systems, Man, and Cybernetics (SMC 2016), 2016, pp. 004277–004282.
[33] T. Zhang, G.H. Golub, Rank-one approximation to high order tensors, SIAM J. Matrix Anal. Appl. 23 (2) (2001) 534–550.
[34] E. Kofidis, P.A. Regalia, On the best rank-1 approximation of higher-order supersymmetric tensors, SIAM J. Matrix Anal. Appl. 23 (3) (2002) 863–884.
[35] A.P. da Silva, P. Comon, A.L.F. de Almeida, A finite algorithm to compute rank-1 tensor approximations, IEEE Signal Process. Lett. 23 (7) (2016) 959–963.
[36] A. Smilde, R. Bro, P. Geladi, Multi-way Analysis: Applications in the Chemical Sciences, John Wiley & Sons, 2005.
[37] W. Sun, L. Huang, H.-C. So, J. Wang, Orthogonal tubal rank-1 tensor pursuit for tensor completion, Signal Process. 157 (2019) 213–224.
[38] D.B. Calvo, Fairness Analysis of Wireless Beamforming Schedulers, Universitat Politecnica de Catalunya, 2004 Ph.D. thesis.